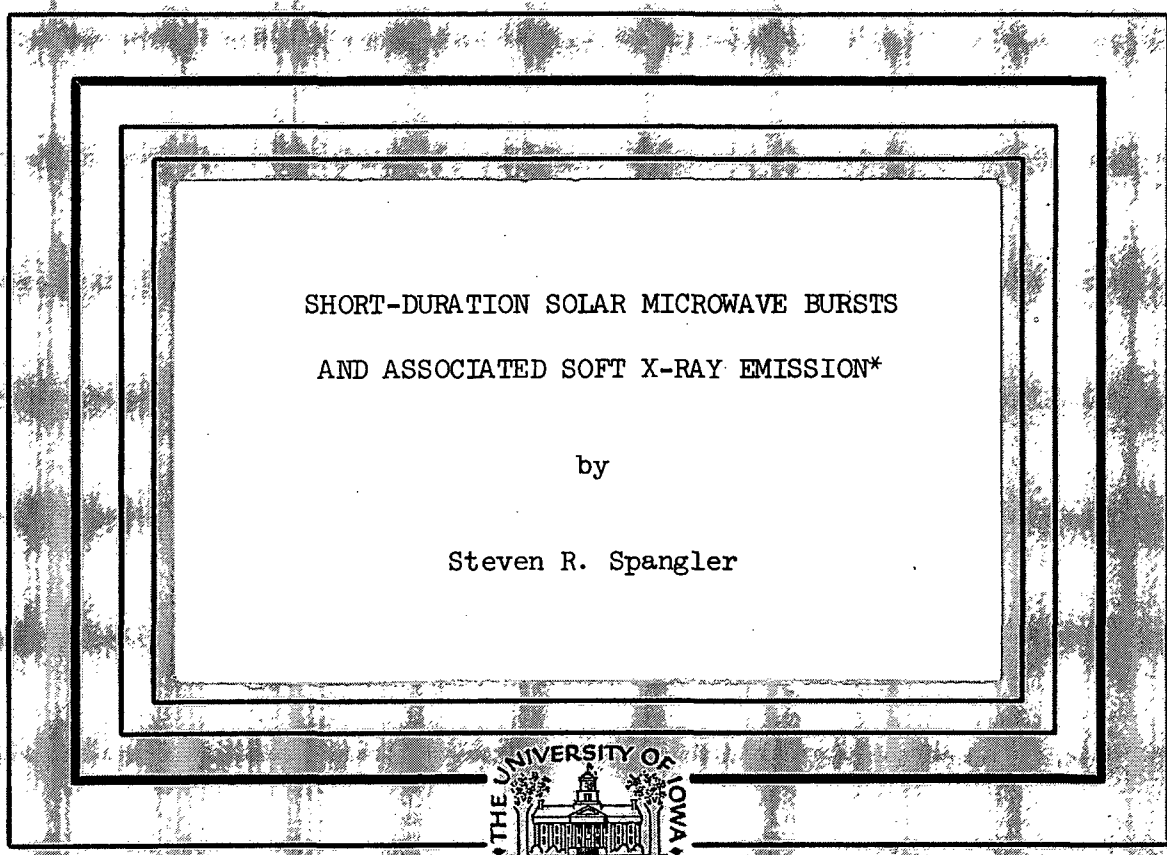


U. of Iowa 73:2
NGL-16-001-002

File as AD-756220



Reproduction in whole or in part is permitted for any purpose of the United States Government.

Research was sponsored in part by the Office of Naval Research under contract N00-14-68-0196-0003.

Department of Physics and Astronomy
THE UNIVERSITY OF IOWA
 Iowa City, Iowa

(NASA-CR-130859) SHORT-DURATION SOLAR MICROWAVE BURSTS AND ASSOCIATED SOFT X-RAY EMISSION M.S. Thesis (Iowa Univ.) 104 p HC \$7.25
 AD-756220 N73-18816
 CACL 03B
 G3/29 64234
 Unclass

SHORT-DURATION SOLAR MICROWAVE BURSTS
AND ASSOCIATED SOFT X-RAY EMISSION*

by

Steven R. Spangler

A thesis submitted in partial fulfillment of the
requirements for the degree of Master of Science
in the Department of Physics and Astronomy
in the Graduate College of
The University of Iowa

December, 1972

Thesis supervisor: Assistant Professor Stanley D. Shawhan

*This work was supported in part by the Office of Naval Research under
contract N00014-68-A-0196-0003 and the National Aeronautics and Space
Administration through Grant NGL-16-001-002.

ABSTRACT

Two hundred and fifty-nine short-duration microwave (15.4 GHz) bursts which occurred during the period of January 1968 to March 1970 were correlated with possible soft x-ray (2-12 Å) flares occurring simultaneously. Sixty-six percent of the microwave bursts which were observed during periods of soft x-ray data coverage had associated soft x-ray flares.

A study of an index of impulsiveness of the microwave flares failed to show a separation of the events into subclasses which could be attributed to distinctly different physical mechanisms.

Consideration of time delays between the onset of the x-ray and microwave flares and between the times of their peak intensities shows that in 61% of the cases the defined start times were within 2 min of each other, with 32% having the defined start times simultaneous within ± 0.5 min. The manner in which the start time of the x-ray burst was defined leads to the conclusion that soft x-ray activity generally preceded the onset of the microwave flare. In 76% of the cases the microwave flare reached peak intensity from 0 to 7 min before the time of the x-ray flux peak. The most probable time difference was 2 ± 0.5 min.

A weak (0.43) correlation was found between the intensities of the microwave and x-ray flares. A very weak (0.15) and statistically

questionable correlation was found between the total energy released in these two energy ranges.

Two models for the electron acceleration mechanism are discussed. An impulsive acceleration mechanism is consistent with delay time observations if the electron density in the soft x-ray flare region is on the order of 10^{10} cm^{-3} . An acceleration mechanism which is continuous over the duration of the microwave flare is necessary if the soft x-ray flare region has number densities of 10^{11} cm^{-3} or higher.

I. INTRODUCTION

The purpose of this study is to investigate the characteristics of short-duration microwave flares and their association with soft (2-12 Å) x-ray emission, and to discuss conclusions concerning the solar flare process which may be inferred from the observations.

Some of the experimental areas to be investigated or commented upon are as follows:

- (1) correlation between microwave and soft x-ray events,
- (2) possibility of classes of short-duration microwave bursts,
- (3) investigation of time morphologies of correlated x-ray and radio bursts, and
- (4) intensity and energy relationships in associated radio and x-ray events.

In addition, we shall discuss the relevance of these observations to models of the flare acceleration mechanism and the processes controlling the rise-and-decay phase of the radio and x-ray flares.

II. THE SOLAR ATMOSPHERE

The solar atmosphere consists of three regions: the photosphere, the chromosphere, and the corona. Below is a discussion of each of these regions and their salient physical characteristics.

A. The Photosphere

The photosphere is the lowest level of the solar atmosphere, and that level which is visible to the eye as the disk of the sun. The gas in the photosphere becomes opaque within a very short radial distance (approximately 400 km), which accounts for the fact that the sun appears as a rather sharp disk.

Densities in the photosphere, compared to regions we shall subsequently be discussing, are rather high. Commonly quoted values are in the range of 10^{17} atoms/cm³. The effective temperature is approximately 5750 K, which accounts for the G2 spectral classification of the sun. Because temperatures in the photosphere are the lowest in the solar atmosphere, the degree of ionization is also the smallest. The photosphere has a general magnetic field of approximately 1 G.

The two most noteworthy phenomena of the photosphere are granulation and sunspots. The granulation is believed to be caused by convection currents bringing hot gases up from the deep interior. Sunspots (phenomena which apparently play an extremely important part in the theory of solar flares) are an example of magnetically

inhibited convection. The sunspots are about 1000 K cooler than the surrounding photosphere, and are the loci of magnetic fields with strengths on the order of thousands of gauss. The great store of magnetic energy which exists in these fields is commonly believed to be the energy source of flares.

B. The Chromosphere

The next highest level in the solar atmosphere is the chromosphere, a narrow zone which extends to a height of approximately 10,000 km above the photosphere. The chromosphere displays the startling property that, contrary to a simple model which would predict cooling with height, its temperature climbs from about 5000 K at the boundary with the photosphere to approximately 1 million K at the boundary with the corona.

This puzzling behavior is one of the most active subjects of solar research (Athay, 1969). Qualitatively it is believed to be due to the conversion of the energy of shock waves propagating through the solar atmosphere into the thermal energy of electrons.

Because of the higher temperature, the degree of ionization in the chromosphere is correspondingly higher than in the photosphere. Densities range from 10^{13} atoms/cm³ at the chromosphere base to 10^{10} – 10^9 atoms/cm³ near the corona. Features of interest found in the chromosphere are spicules, prominences, plages, and flares.

C. The Corona

The final layer of the solar atmosphere is the corona. The corona is the highly-ionized outer layer of the solar atmosphere which is seen as a milky halo about the sun during a period of total solar eclipse. The corona begins at about 10,000 km above the photosphere and has no well-defined upper limit. It is generally considered to simply become an ever more tenuous, high-velocity plasma known as the solar wind. At the earth this stream has a velocity of approximately 480 km/sec. Closer to the sun the corona is typified by high temperatures on the order of 10^6 K and low electron densities which range from 10^8 — 10^9 cm^{-3} at the chromosphere base to 10^3 cm^{-3} at 3 solar radii. The corona is characterized by total ionization of hydrogen and helium.

One coronal feature of note is the coronal condensation. The electron densities of these condensations are approximately ten times the regular coronal densities at the heights at which they occur, and the temperatures are also elevated. Since condensations are associated with active regions, their temperature and density anomalies are of interest to the theory of solar flares.

A model of the solar atmosphere which shows electron density and temperature as a function of height is shown in Figure 1 (Van de Hulst, 1950).

III. THE SOLAR FLARE

A. Flare Models

The solar flare is one of the most catastrophic processes which occur in the solar system. A typical flare releases on the order of 10^{32} erg in its lifetime, which can be as short as a few minutes.

A feature common to nearly all flare models is the requirement that the energy involved is stored in the magnetic field of the flare region (De Jager, 1969). This is due to the fact that flares are always observed occurring along lines of magnetic neutrality separating two regions of opposing magnetic polarity. These are regions where the vertical component of the B field is zero and the horizontal gradient dH/dZ is large.

It has been shown (De Jager, 1969) that the magnetic energy in a flare region is sufficiently great to produce the energy released by a solar flare. The energy released when a region of volume V and magnetic field B_1 reduces its magnetic field to B_2 is

$$\Delta E = \frac{[B_1^2 - B_2^2]}{8\pi} V$$

We find that for a volume of 10^{28} cm^3 a reduction in field strength from 500 to 410 G, or a reduction from 300 to 100 G, will release

approximately 3×10^{32} erg. Since flares are observed to have such values of volume and magnetic field the magnetic energy hypothesis seems entirely adequate.

The mechanism by which the solar flare is triggered is obviously a more difficult question. Currently in favor is a theory developed by Alfvén and Carlqvist (1967) based on the phenomenon of current limitation in plasmas. [See also Carlqvist (1969).] It is a well-known phenomenon in electrical circuit technology that if a circuit in which current is flowing is broken the energy contained in the circuit is released at the point of interruption. The current-limitation effect in plasmas is the observed nonconductivity of plasmas above a certain value of the current passing through them. At this point the plasma becomes essentially a break in the circuit. The Carlqvist model assumes force-free currents flow along the magnetic field lines in the active regions. When the limitation current is reached, a break is formed and the "circuit energy" of the active region is released. That very large currents (on the order of 10^{11} amps) exist in flare regions has been observationally established (Severny, 1969). The Carlqvist mechanism provides an attractive mechanism for the production of electrons associated with the flash phase of a flare.

A recent criticism has arisen based on the work of Smith and Priest (1972). They contend that before the Carlqvist instability

takes place, the ion sound instability occurs, dissipating the circuit energy in the creation of turbulence which just heats the electrons and does not allow the formation of a large electric field.

A serious objection to this theory is that while the ion sound instability may be able to explain such thermal phenomena as the H α flares, soft x-ray bursts, and gradual rise-and-fall microwave flares, it is incapable of explaining the important phenomena which are obviously nonthermal in nature. These include the impulsive hard x-ray bursts and impulsive microwave bursts.

B. Flare Regions

The regions in which the visible, or H α , flares occur and the regions where the radio and x-ray emission originate are significantly different. The H α flare originates in a rather cool, dense plasma with temperatures on the order of 10^4 K and electron densities on the order of 10^{13} cm $^{-3}$. In contrast, the phenomena of interest to this study, x-ray and microwave radiation, originate in a tenuous, extremely hot plasma entirely inconsistent with the physical parameters of the optical flare. Parameters listed for the region of these radiations are generally agreed (Drake, 1970; Hudson et al., 1969a, 1969b) to be electron densities on the order 10^9 — 10^{11} cm $^{-3}$ and temperatures on the order of 10^7 K. The location of this energetic plasma is generally believed to be in the lower corona or upper chromosphere above the optical flare. A commonly quoted model for the structure of this region will be given later.

C. Centimetric Wavelength Emission

Kundu (1965) presents three classifications for radio bursts at centimetric wavelengths. These classifications are shown in Figure 2. Type A bursts are often referred to as impulsive bursts. They are characterized by durations of less than 10 min and a rapid rise to and decay from the maximum. Kundu quotes brightness temperatures on the order of 10^8 — 10^9 K. About 60% of such bursts display circular polarization. Type B bursts show a fairly rapid rise to the maximum followed by a slower decay. The rise time is on the order of several minutes, and the decay time on the order of 10's of minutes. Type C bursts are referred to as the GRF- (gradual rise and fall) type bursts. They show a low profile, and their time signature is characterized by both a slow rise to maximum and a slow decay.

Type A bursts, as stated above, are referred to as the microwave impulsive bursts. Types B and C are referred to as the long-enduring microwave flares. By far the most popular theory for the mechanism of the impulsive bursts is that they are caused by gyro-synchrotron emission from a nonthermal electron distribution, although different models including thermal bremsstrahlung, nonthermal bremsstrahlung, and a combination of thermal radiation with gyro-synchrotron emission have been advanced. Types B and C bursts are accounted for by a thermal mechanism, with the type B bursts perhaps also having a magnetic bremsstrahlung component.

D. X-Ray Emission From the Sun

X-ray bursts from the sun have been classified into two classes: nonthermal and quasi-thermal (De Jager, 1967b). The basis for the distinction is photon energy. Bursts of photon energy greater than 10 keV are termed nonthermal, and those of photon energy less than 10 keV are termed quasi-thermal. The rationale for this system is the fact that x-ray bursts at energies greater than 10 keV are accounted for by nonthermal bremsstrahlung (De Jager, 1967b). On the other hand, x-ray bursts of energy less than 10 keV have been consistently accounted for by free-free emission from a Maxwellian electron ensemble with temperatures on the order of 10^7 K. There is an exception to the above statement. Hard ($E > 10$ keV) x-ray bursts have two classes: the impulsive x-ray bursts and the long-enduring, gradual rise and fall analagous to the case for bursts on centimetric wavelengths. The gradual rise-and-fall component seems consistent with thermal bremsstrahlung (Kane, 1969), while the impulsive component is attributed to nonthermal bremsstrahlung. Considerable debate has arisen as to the nature of the hard x-ray bursts, with some arguments being raised to support a thermal mechanism. Takakura (1969c) has shown the plausibility of a compound process combining both the mechanisms.

E. Comparison of Microwave and X-Ray Bursts

The comparison of simultaneous x-ray and microwave emission from solar flares has been the subject of considerable research in the last ten years. Work done previous to 1965 is given an excellent

review by Kundu (1965). The comparison between microwave impulsive bursts and hard x-ray bursts has been investigated in a number of papers (Arnoldy, Kane, and Winckler, 1968; Hudson, Peterson, and Schwartz, 1969c) which reported observations in a wide range of radio frequencies and x-ray energies.

The most striking observational fact is the extremely close similarity between the time profiles of the two bursts. This strongly suggests that the bursts are caused by the same energetic electrons. Takakura (1969a) has shown both types of flares are consistent with a nonthermal electron distribution represented by a power law distribution with indices in the range from 3 to 5. Takakura believes that the emitting regions cannot be the same due to the fact that if the same electrons were responsible for both the x-ray and radio flare (identical source region), the radio flux should be 10^3 to 10^4 times as intense as is observed. He therefore advances the model shown in Figure 3. This model assumes that the regions marked R, regions denoted by low electron densities ($10^8 - 10^9$ electrons/cm³) and high magnetic fields (approximately 500 G to 1000 G), are responsible for the centimetric radio emission, while the larger region marked X, which is typified by higher number densities and small magnetic fields, is the region of origin for the long-enduring microwave flare, the soft x-ray flare, and the impulsive x-ray burst.

Takakura's model has been supported by high resolution interferometric observations of impulsive microwave flares which do indeed show that the centimetric emission comes from two regions separated

by about 1 min of arc (Tanaka et al., 1967). Takakura's model is able to explain the radio x-ray number discrepancy by assuming the number density of energetic electrons is higher in region X. The basic feature of Takakura's model is the autonomy of the radio and x-ray emitting regions.

Holt and Ramaty (1969), on the other hand, have presented calculations supporting the contention that the emitting regions are the same, and that the observed number discrepancy is due to gyro-synchrotron self-absorption, which had not been adequately considered previously. Thus a common emitting region might be a possibility. A single region model advanced by Vorpahl (1972) is shown in Figure 4. In this model the hard x-ray burst and the microwave impulsive burst occur in the same region, and the discrepancy in the number of emitters is resolved by gyro-synchrotron reabsorption. Another distinction of the Vorpahl model is that the flare is located at a much lower altitude (in the lower chromosphere) than in the Takakura model. This is consistent with recent measurements by Zirin et al. (1972) of flare heights on the basis of low-frequency cutoffs in microwave spectra.

Several studies have considered the relationships between long-enduring microwave flares and soft x-ray flares (Shimabukuro, 1970; Wende, 1968; and Acton, 1968). Wende (1968) considered this problem using data of the same form as the present thesis. There is agreement in all such studies that the mechanism responsible for both

bursts is free-free emission (thermal bremsstrahlung), although the emitting regions are probably different (Shimabukuro, 1970).

Studies comparing microwave impulsive bursts and soft x-ray bursts are much less numerous than the studies mentioned above due to the fact that the mechanisms responsible are generally assumed to be dissimilar. Teske and Thomas (1969) have studied the correlation between 8–12 Å x-ray bursts and radio bursts at 2700 MHz. Another study carried out by Culhane and Phillips (1970) correlates x rays of energy less than 10 keV with single-frequency radio bursts. Their study has the advantage of spectral information within this range. McKenzie (1972) has considered the correlation between x-ray bursts in several energy ranges above 7 keV with centimetric radio bursts. The main effort of the paper was directed toward an understanding of the flare acceleration mechanism by comparison of the x-ray flux in different energy ranges. The findings of these investigations will be compared in some detail to the present thesis in chapter VI.

In many ways the scope of this study is similar to that of Teske and Thomas (1969) and Culhane and Phillips (1970) in that we consider the association of soft x-ray bursts and short-duration microwave bursts. Some of the differences are:

- (1) Whereas in the two previous studies the x-ray flares were the control group, in this study the microwave flares are the control group.
- (2) The number of events considered is greater in this study.

- (3) The microwave frequency monitored is higher than in the two previous studies, and the x-ray energy range monitored is different from that of Teske and Thomas.

The goal of this thesis will be to first present observational findings concerning the short-duration bursts and their associated x-ray emission. Some of these findings will be original; others will be confirmation of earlier findings [especially those of Teske and Thomas (1969) and Culhane and Phillips (1970)] with a large data body. Having obtained these observational characteristics an attempt will be made to find a model for the flare acceleration mechanism which is consistent with the data and with observations of other flare-related phenomena.

IV. INSTRUMENTATION AND EVENT

SELECTION CRITERIA

Three experiments provided the observational data for this study. The first was the 15.375 GHz radiometer of the University of Iowa North Liberty Radio Observatory (NLRO). The second was the University of Iowa twin soft x-ray experiments aboard the earth-orbiting satellite Explorer 33 and the moon-orbiting satellite Explorer 35. Finally, data were taken from the list of solar bursts observed by the Air Force Cambridge Research Laboratory's Sagamore Hill Radio Observatory radiometers which operate over a frequency range of 260 MHz to 15,400 MHz.

A frequency of 15.4 GHz was chosen because it is one of the highest frequencies at which continuous data coverage is available. A high frequency in the centimetric range is desirable because radiation emitted deep in the solar atmosphere near flare regions is less attenuated by overlying matter, and nonthermal effects are predominant over thermal phenomena.

A. The University of Iowa 2 cm Radiometer

The 15.373 GHz radiometer (Wende, 1968) is an equatorially-driven paraboloid with a dish diameter of 4 ft and a beam width of 1°. The antenna feed is of the Cassegrain type, and the detection system employs a Ryle-Vonberg receiver (Kraus, 1966). The advantage

of such a system is that it eliminates false events due to receiver-gain fluctuation.

The radiometer output is recorded on magnetic tape, using a voltage-controlled oscillator (VCO), and on strip charts. The charts are generally calibrated in terms of VCO frequency and antenna temperature.

One of the great difficulties encountered by this project is that subsequent calibration curves do not show internal agreement. This implies that the response of the system changed over the two and one-half years of radiometer operation.

Also, there seem to be random pointing errors which cannot be adequately corrected. The inconsistency between the "corrected" NLRO and Sagamore Hill flux values are pointed out in Table 2. Consequently, the NLRO data are not used for absolute flux determinations. As is, the NLRO data is still usable for the observation of occurrences and the determination of event times, flare durations, and time-delay correlations with soft x-ray data.

B. The University of Iowa Explorer 33 and 35

Solar Soft X-Ray Experiment

The University of Iowa soft x-ray experiment (Van Allen, 1967) consisted of two identical instruments aboard the spacecraft Explorer 33 and Explorer 35. Each experiment consisted of three Eon-type 6213 Geiger Müller tubes with thin mica windows which allowed passage of soft (2-12 Å) x rays. The spacecraft reported the soft x-ray

flux from the sun at 82-sec intervals in the case of Explorer 35 and 164-sec intervals in the case of Explorer 33.

For the purposes of this study three forms of the data were utilized: the tabulated data giving x-ray flux as a function of time, plots of x-ray flux graphed in 12-hour periods, and the University of Iowa x-ray burst catalog. The flares were, for the most part, drawn from the x-ray burst catalog. The x-ray burst catalog is a computer-generated listing of x-ray events which covers the time period from the launching of Explorer 33 (June, 1966) to August 14, 1969. The tabulated data form gives the 2-12 Å flux as a function of date and universal time. The tabulated data were used to determine soft x-ray flux change. Finally, the soft x-ray flux plots were used as a visual check on each event to search for irregularities or inaccuracies in the soft x-ray burst catalog, and to investigate those cases for which the catalog listed no x-ray burst to determine whether the absence was real or due to a gap in the received data. Examples of the x-ray flux plots are given in Figures 5 and 6.

C. The Sagamore Hill Radio Observatory

The Sagamore Hill Radio Observatory at Hamilton, Massachusetts is operated by the Air Force Cambridge Research Laboratories (AFCRL). Sagamore Hill, in 1966, began a daily patrol of the sun at 8800, 4995, 2695, 1415, and 606 MHz. The patrol was extended in late 1967 to 15,400 MHz. The 15,400 MHz system consists of a 3 ft diameter

paraboloid mounted on a equitorial drive. The accuracy of flux measurements is approximately 5% at 606 to 1415 MHz and 5 to 10% at the higher frequencies (Castelli and Michel, 1967). All receivers are of the Dicke system variety which minimizes error due to receiver-gain fluctuation. All data are corrected for atmospheric attenuation and are normalized to one astronomical unit. The latter effect amounts to approximately 1% to 3%.

D. Event Selection Criteria

Using the NLRO data, any event which rose three standard deviations above the RMS fluctuations of the background noise and which was of 10 min duration or less was categorized as an event. The start time was defined as that time when the signal rose more than one standard deviation out of the noise; the peak time as the time when the amplitude reached a maximum; and the end as that time when the declining flux once again reached the 1σ level. Flare durations were defined as the end-minus-start time. Time was judged to be accurate to better than 0.5 min.

The Sagamore Hill values were obtained from their catalog of solar bursts. Listed on the data sheets were the start and peak time of each event, the flare duration, the peak to pre-flare flux change, and the mean or average flux change. In selecting events all events were chosen whose duration was less than 10 min, and whose morphological profile classified it as a simple 1, simple 2, or simple 3 burst. The different burst types are shown in Figure 7

(Kundu, 1965). Other morphological types, such as complex flares or those with post-burst increases, were not used due to the fact that such parameters as decay time, duration, and mean flux would be distorted, and that in most cases the complicated structure would be due not to the flash-phase phenomenon of interest but most likely be a gradual rise-and-fall event associated with the soft x-ray flare. Soft x-ray bursts were considered correlated with the microwave flare if the radio burst occurred during the x-ray flare.

For the bursts observed at Sagamore Hill data were available at more than one frequency. When a x-ray flare was identified the start time was defined as that time when the x-ray flux rose to a value of 20% above the pre-flare background flux. The end time was similarly defined as being when the soft x-ray flux declined to a value 20% above the background flux. Values of the soft x-ray peak to background flux were determined from the tabulated data. The procedure was to take the mean of the ten data points preceding the flare catalog-determined start time. The peak flux change was then defined as the maximum of the x-ray flux minus the mean pre-flare flux. In a few cases this procedure could not be followed as the soft x-ray burst associated with the microwave flare occurred less than 820 sec (time for ten data points) after the end of a previous x-ray event. In these cases as many points as possible were taken which subjectively constituted the pre-flare flux. It is estimated that this process did not result in errors of greater than 10%.

The SUMF, or total energy integral, was the result of a numerical summation performed by the computer in the x-ray burst catalog. The units of this parameter are erg/cm^2 . It should be noted at this point that the comment "flare exists, data discontinuity" reported in the x-ray data for some events refers to those cases for which the plots show a data gap occurring during a flare such that the important correlation parameters such as peak time, flux change, and SUMF could not be estimated.

Figures 8 through 10 show the time histories of several events observed at the NLRO for which soft x-ray flares are correlated. The lower record represents the actual chart record of the event while the data points above the chart record represent the 2-12 Å x-ray flux at regular time intervals. It is to be noted on events 8 and 10 that a lower-lying radio enhancement whose time profile is similar to that of the x-ray burst is observed. These low-profile flares are presumed to be thermal emission. These enhancements comprise the microwave counterpart of the thermal soft x-ray flare. They are to be contrasted with the impulsive bursts which have time profiles which are completely different than the soft x-ray time profile. This is a strong indication that the impulsive bursts are nonthermal in nature.

V. PRESENTATION OF EXPERIMENTAL RESULTS

A. Event Statistics

This section presents the findings of this study concerning short-duration microwave bursts and their association with soft x-ray emission. Table 3, sections A through D, lists the events which comprise the body of data. It will be noted that those bursts observed at NLRO are segregated from those observed at the Sagamore Hill Radio Observatory. This is due to the flux-change discrepancies alluded to in chapter IV. All relationships involving microwave intensity have therefore used only Sagamore Hill flux-change values for concurrent events. This is done for the sake of consistency in the results. Other relationships which do not require a knowledge of the microwave flux utilize the NLRO and Sagamore data interchangeability.

Table 3-A lists the fifty-six events observed at the NLRO. Listed for each event are the date, start, peak and end time, and flux-change measurement as described in chapter IV. Table 3-B lists the presence or absence of soft x-ray activity during the time of each of the bursts listed in Table 3-A. If a flare occurred at that time its parameters were listed. These parameters were the start, peak and end time, total x-ray energy in ergs/cm^2 received by the satellite during the flare (SUMF), and peak flux

change in milli-erg $\text{sec}^{-1} \text{cm}^{-2}$. If an x-ray flare was not observed coincidentally with the microwave bursts the Explorer 33 and 35 x-ray flux plots were consulted to determine whether this was due to a data gap or a real absence of activity. Which of these two situations was applicable is indicated for those cases. Tables 3-C and 3-D are identical to 3-A and 3-B except reference is now made to those events observed at Sagamore Hill. In addition, the format of Table 3-C differs slightly from 3-A. Parameters listed in Table 3-C are the start and peak times, burst duration, peak flux change, mean flux change, and burst morphology, whether the bursts was a simple 1, simple 2, or simple 3 type burst as defined previously.

Of the observed total of 259 microwave bursts, 146 were found to have associated soft x-ray emission. Of the remaining 113 events 39 occurred during soft x-ray data gaps. Seventy-four were found which were not associated with x-ray events. If we consider only those radio flares which occurred during a period of soft x-ray data coverage, we find that 146 out of 220, or 66%, of all such events had accompanying soft x-ray emission. In the studies by Culhane and Phillips (1970) and Teske and Thomas (1969) the x-ray flares rather than radio flares were used as the control group. Culhane and Phillips did attempt correlating x-ray bursts with radio bursts, but they considered flares at any radio frequency. This is obviously a more general class than centimetric impulsive bursts. In their investigation they found all but 1 of 38 radio flares occurred during periods of x-ray activity, and 26 of the 38 radio flares had associated x-ray flares.

To obtain the peak intensity distribution of the microwave flares we use the Sagamore Hill classification scheme (Castelli and Guidice, 1972):

0 to 50 flux units --- class 1

50 to 500 flux units --- class 2

> 500 flux units --- class 3 .

A table giving the population of each class is given in Table 1.

The diagram shows a sharp drop off of frequency of occurrence with increasing intensity as class 1 has far more events (39% of total) than the other two classes combined (11% of total). The table would seem to indicate that increasing radiometer sensitivity would greatly increase the number of such events observed.

It is worth noting that soft x-ray flares are far more numerous than microwave impulsive bursts with present radiometer sensitivity. Soft x-ray bursts occur typically several times a day, whereas the type of radio event of interest to this study occurred with a frequency of less than one per day.

Table 1

Population of intensity classes

<u>Class</u>	<u>Number of Cases</u>
1	186
2	22
3	1

B. Morphologies of Short-Duration Microwave Bursts

One of the first experimental questions which should be asked is whether the selection criteria for microwave bursts was too liberal. That is, by employing only a duration criterion have we allowed more than one class of flares which owe their origin to distinctly dissimilar physical mechanisms?

Following the procedure of Kundu (1965) for the identification of subclasses, the flux change and duration for all flares observed at the Sagamore Hill Observatory is shown in Figure 11. There are no apparent subclasses distinguished by intensity-duration grouping. A more sensitive test of this point occurs if a histogram is made of the following parameter:

$$[\text{Flare Flux Change/Flare Duration}] \quad ,$$

which may be considered an index of impulsiveness. If more than one class of flares exists each subclass might be expected to have a peak corresponding to it on the histogram. Such a diagram for the events under consideration is shown in Figure 12.

The events show a distribution of about one peak corresponding to an impulsiveness index of about five. No evidence is seen for the existence of a second class.

An additional interesting observation is shown in Figure 13, which is a histogram of the microwave flare durations for all events observed at both observatories. Two facts from this diagram are noteworthy. The first is the maximum between 1 and 2 min corresponding to the most probable value the duration can have for this set of

flares. Seventy-five out of 259, or 29%, of the microwave flares had durations in this range. The second feature of note is the drop-off of frequency of occurrence with increasing duration. This effect is stronger for events of duration less than 4 min. One hundred and ninety-five flares, comprising 75% of the total, have durations of 4 min or less.

C. Microwave—X-Ray Delay Times

Figure 14 gives the frequency histogram for peak-to-peak delay times, and Figure 15 gives the histogram for start-to-start delay times. These parameters are defined as follows: the start-to-start delay time is the time in minutes between the onset of the radio flare and the onset of the x-ray flare. The delay time is given a negative value if the x-ray emission began first, and a positive value if the microwave flare began first. The peak-to-peak delay time is defined as the difference in time from the time of peak microwave flux to the time of peak x-ray flux. Again, the delay time was assigned a negative value if the x-ray flare peaked before the microwave flares, and a positive value if the microwave flare reached peak flux first.

In Figure 15 it is seen that although there are a great number of cases in which x-ray activity far precedes the microwave burst, in 61% of the cases the defined start times are within 2 min of each other with 32% of the cases at 0 ± 0.5 min. Before making statements about the time development of the x-ray and microwave radiation

processes on the basis of this diagram it must be noted that the time delays plotted are the differences in time between the start of the microwave burst and the defined start of the soft x-ray flare. In this study the criterion used by Drake (1970) was applied which defined the start of the x-ray flare as that time when the rising x-ray flux rose to a value 20% above the pre-flare background. Due to the slow (at least several minutes) rise time of the soft x-ray bursts Figure 15 would seem to imply that in most cases the soft x-ray emission began several minutes before the microwave burst.

A visual inspection of the flux plots of a number of x-ray flares demonstrated that this was indeed the case. A comparison between the defined start time and a subjective start time determined by the author's opinion of when the x-ray flux curve changed slope showed that for small x-ray flares (Δs on the order of several milli-ergs $\text{sec}^{-1} \text{cm}^{-2}$) the subjective start time preceded the defined start time by 1 to 3 min. For large x-ray bursts (Δs on the order of tens of milli-ergs $\text{sec}^{-1} \text{cm}^{-2}$) the subjective start time preceded the defined start time by 4 to 6 min.

Figure 14 presents the interesting result that although in most cases x-ray emission precedes the onset of the microwave burst, in 133 out of 147, or 91%, of the cases the microwave burst peaks simultaneously (± 0.5 min) or before the x-ray peak. In 80% of the cases the delay time is in the range of 0 to 7 min. As is clear from Figure 14, the most probable delay time is 2 ± 0.5 min. The

conclusion to be drawn from Figures 14 and 15 is that although the process producing the soft x rays is operating before that producing the impulsive microwave burst, the process producing the short-duration microwave flare typically reaches peak activity and begins to subside several minutes before the process producing the soft x rays reaches peak activity.

The results of Figures 14 and 15 agree with the conclusions of Teske and Thomas (1969) and Culhane and Phillips (1970) but present many more cases than previously considered. A more thorough discussion and a comparison of results are given in chapter VI.

D. Microwave—X-Ray Amplitude and Energy Relationships

One of the most important experimental relationships in terms of identifying mechanisms responsible for observed emission is a plot of the intensity in one wavelength range to its intensity in another energy region. In this section we consider the relation between microwave flare flux change (in solar flux units) and the soft x-ray flux change (in $\text{milli-erg sec}^{-1} \text{ cm}^{-2}$) for those flares observed at Sagamore Hill.

Two previous studies have considered this point. Culhane and Phillips (1970) found no relationship between the two fluxes while Teske and Thomas (1969), with a smaller number of cases, found evidence for a positive correlation between the two intensities. The results of the present study are shown in Figure 16.

Although there is an indication of a positive correlation, a definite pronouncement requires a quantitative measure of the correlation. A computer program was developed which fit data to a straight line on a log-log plot, determining by least squares the slope and intercept of the line, and then calculating the correlation coefficient of that linear relationship.

The least squares fit curve to Figure 16 gave an intercept of $1.7 \text{ milli-ergs sec}^{-1} \text{ cm}^{-2}$, and a slope of 0.39. The correlation coefficient for this relationship was 0.43. To test if this value of the correlation coefficient was significant, the following "experiment" was undertaken. One hundred and seven random data pairs (the number 107 chosen to coincide with the number of points in Figure 16) were submitted to the computer program which analyzed the data from Figure 16. The program was run 5 times, each time using a different random data set. The correlation coefficients obtained ranged from 0.0 to 0.05. The fact that the correlation coefficient obtained for the flux-flux relationship was nearly an order of magnitude greater than the maximum correlation coefficient obtained from random data sets is strong evidence that the correlation is significant.

In addition, Young (1962) states that for a body of 100 data pairs a correlation coefficient of 0.327 represents a 99.9% confidence that the correlation is real. The confidence that the correlation found above is real is therefore greater than 99.9%. For comparison, the flux-flux data of Teske and Thomas (1969) was submitted to the

same analysis. This was done by scaling data off Figure 3 of their paper. The least squares fit to their data gave an intercept of 4.3 milli-ergs $\text{sec}^{-1} \text{cm}^{-2}$ and a slope of 0.45. The correlation coefficient for the relationship was 0.63. Again, the random data experiment was carried out, this time with 40 data pairs. The number in the plot by Teske and Thomas was 41. The range of the correlation coefficient obtained was 0.00—0.16. Again, the observed correlation coefficient far exceeds that obtained from a random body of data. Young (1962) gives a value of 0.502 for the 99.9% confidence level for the correlation coefficient if the data body consists of 40 data pairs. The confidence in the relationship found by Teske and Thomas is therefore greater than 99.9%.

In comparing the relationship between fluxes found by Teske and Thomas (1969) with that of this thesis, it is seen that although the relationship found in this study is weaker, the form of the relationship is similar.

Another relationship which might prove of interest is a comparison of the total energy released in the radio flare to the total energy released in the x-ray flare. Although a meaningful physical interpretation of such a relationship may seem somewhat vague, Arnoldy, Kane, and Winckler (1968) found a stronger correlation between these parameters than between the peak flux excess when considering the relationship between microwave impulsive bursts and hard (10—50 keV) x-ray bursts. The soft x-ray energy was taken

as the SUMF parameter previously described, and the microwave energy was taken to be the mean flare flux multiplied by the flare duration in minutes and the constant 60 (the number of seconds in a minute) to provide consistent units.

The results are displayed in Figure 17. The data was again submitted to computer analysis. The least squares fit gave an intercept of 7.3 ergs/cm^2 , a slope of -0.13 , and a correlation coefficient of 0.14 . For a data ensemble of 90 points, the level of 90% confidence is a correlation coefficient of 0.188 . The confidence that a relationship does exist between these parameters is therefore less than 90%, and should be considered uncertain.

A summary of the statistical analysis of the flux-flux and energy-energy data is given in Table 4.

VI. INTERPRETATION OF EXPERIMENTAL RESULTS

In this chapter attention will be concentrated on the discussion of two important points:

- (1) a qualitative model of the solar flare acceleration mechanism and the related question of energetic electron lifetimes in physical conditions found in solar flares, and
- (2) interpretation of the phenomena discussed in chapter V of this study in the context of this model.

A. Schematic Description of Flare Process

We shall assume that outside the region which actually emits the detectable radiation an instability occurs before the onset of the flare. We also make the assumption that the region in which the instability occurs is connected by magnetic field lines to the region in which the detectable flare will occur. When the instability occurs electrons are accelerated to high energies and travel down the field lines to the flare region. It is assumed that the principle source of the flare energy is contained in these energetic electrons.

The above assumptions are consistent with the flare initiation models of Carlqvist (1969), Syrovatskii (1969), and Sturrock and Coppi (1966).

The detected flare radiation originates from this energetic electron ensemble in the following manner. When the energetic particles encounter the strong magnetic fields in the chromosphere, they

begin to radiate gyro-synchrotron radiation which is detected as the short-duration microwave burst. These same energy electrons impacting on the matter of greater ion density in the chromosphere produce the nonthermal Bremstrahlung responsible for the hard x-ray burst and the impulsive component of the HX flare (Vorpahl, 1972). In a time determined by the ion density in the soft x-ray flare region these energetic electrons thermalize, thus heating up the flare region, which accounts for such thermal phenomena as the soft x-ray flare (McKenzie, 1972) and the gradual rise-and-fall microwave bursts.

B. Model of the Solar Flare Acceleration Mechanism

A schematic form of the flare acceleration mechanism is given in Figure 18. The lower of the two diagrams represents the time-varying acceleration mechanism. The diagram at the top shows a hypothetical flare in which associated short-duration microwave and soft x-ray emission are present. This event has the typical characteristics of x-ray emission beginning slightly before the start of the microwave burst, but the peak of the microwave emission preceding the soft x-ray peak by approximately 2 min.

We assume the behavior of the acceleration mechanism is as follows. The mechanism begins by accelerating particles of low energy, less than 1 keV. By the time t_1 , the time when an increase in the soft x-ray emission has begun, it is accelerating particles in the energy range 1-6 keV. By the time t_2 it is accelerating electrons to energies of E_s , where E_s is the energy of electrons

sufficiently energetic to produce significant microwave radiation. This energy is naturally dependent on the strength of the magnetic field in the microwave flare region. In Takakura's model, which assumes magnetic fields in the 500—1000 G range, E_s is of the order of 10 keV. If the magnetic field is in fact closer to 200 G, E_s would naturally be larger, perhaps in the range 50—100 keV. At the time t_3 the acceleration mechanism is accelerating electrons to the maximum energy to which they will be accelerated, which is probably in the range 500—1000 keV (Takakura, 1969b). The time t_3 represents the time of the maximum number of highly energetic electrons in the flare region. Time t_3 therefore corresponds to the time of maximum microwave emission. After time t_3 two possible time developments might occur. If the collisional thermalization time is very short compared to the burst decay time, the acceleration mechanism will follow the course indicated in Figure 18, that is, it will begin to accelerate less and less energetic electrons until, at time t_4 when the maximum accelerated particle energy drops below E_s , no further impulsive microwave emission will be observed. If the particle thermalization time is comparable to the flare decay time, however, the acceleration mechanism may stop when it reaches maximum energy, i.e., time t_3 . Subsequent phenomena would then be due strictly to the thermalization of the energetic particles accelerated before and up to time t_3 . An understanding of the time of peak soft x-ray emission is not so obvious, however, and a discussion of this topic is deferred to the next section of this chapter.

C. Relation of Experimental Findings
to Flare Acceleration Model

In the last section we advanced the model of a flare acceleration mechanism in which electrons are accelerated to ever greater energies until, at a time corresponding to the peak of the microwave flare, particles are being accelerated to the maximum energy to which they will be accelerated. After this the mechanism accelerates the electrons to progressively smaller energies, until acceleration ceases. The time lag between maximum energy acceleration and no acceleration may vary between zero time and the actual decay time of the flare, depending on the efficiency of thermalization mechanisms in the flare region.

In this section we wish to interpret the observational findings of Chapter V in relation to this mechanism, and to see if the findings allow any insight into characteristics of the mechanism. We shall discuss the results in two sub-sections: interpretations of delay times and flux and energy relationships.

1. Interpretation of Delay Times

As stated in Chapter V, the investigation of microwave x-ray start times showed the following characteristic. Although in many cases the defined start times of the soft x-ray flare began many minutes earlier than the onset of the microwave burst, the great majority of events tended to have (within detector time resolution) flare onsets within 1 or 2 min of each other, with a very pronounced peak at zero time delay. It is very important to remember, however,

that the start time was defined as when the increasing x-ray flux rose 20% above the pre-flare background. Given the rather slow (at least several minutes) rise time of most soft x-ray bursts it becomes clear that in most cases the onset of soft x-ray activity begins prior to the microwave burst. This is consistent with the previous work of both Teske and Thomas (1969) and Culhane and Phillips (1970). Teske and Thomas, studying x-ray flares in the range 8–12 Å, found that when they operated their detector in the low sensitivity mode the centimetric burst and the x-ray burst generally began within 1 min of each other. When the detector was operated in the high sensitivity mode, however, they found that without exception the x-ray event began several minutes prior to the microwave burst. Culhane and Phillips found x-ray activity could frequently be detected before the start of the microwave burst and before the rapid rise of the x-ray flux. Agreement thus emerges from the three studies that the soft x-ray activity most probably begins several minutes before the onset of the microwave flare. In terms of the model advanced in Figure 18 it is clear that this period corresponds to the time t_1-t_2 , in which the acceleration mechanism is accelerating electrons to energies less than E_s . It seems that this phase would last anywhere from several minutes to less than 1 min. If this is indeed the case one would expect the low-energy nonthermal x rays ($10 \text{ keV} < h\nu < 20 \text{ keV}$) to commence shortly before the microwave burst. To the best of the author's knowledge this determination has not been made.

In the case of those events in which x-ray emission far precedes (> 10 min) the microwave burst one wonders if the explanation is that the t_1-t_2 phase of the acceleration mechanism is unusually long, or whether in those cases the long pre-flare activity is due to pre-burst heating and compression of the flare region. Investigation of the flux-curve slope as a function of time might be revealing in this context. The t_2-t_3 stage time duration is simply related to the rise time of the microwave burst.

Having discussed start-to-start time delays, consideration is now given to the peak-to-peak delay times. In understanding the observed peak-to-peak delay time attention is drawn to the fact that the cooling time for an x-ray flare region, due to radiative cooling or conduction along magnetic field lines, is a time long compared to the energy input time of the nonthermal electrons. We shall therefore consider the soft x-ray flare region as effectively insulated during the time when the acceleration mechanism is operative.

As stated in Chapter V, the result of this study concerning the peak-to-peak delay times was as follows. The great majority of flares had peak-to-peak delay times in the range of 1-7 min, with a maximum probability of 2 min (the microwave peak, of course, preceding the soft x-ray peak). Teske and Thomas (1969), using x-ray data in the 8-12 Å range, found delay times to be typically 3-6 min. Since this study used 2-12 Å x-ray data, the difference between the present study and that of Teske and Thomas may be interpreted

as being due to the softer x rays peaking later than the harder x rays. This suspicion is indeed confirmed by Culhane and Phillips (1970), who could study events in several energy ranges under 10 keV. They found that the harder the radiation, the earlier the peak came after the microwave burst peak. Agreement thus emerges from the three studies as stated below.

In general, the peak of the soft x rays will tend to come several minutes after the microwave flare peak. The peak time is energy dependent in the sense that the harder radiation emission tends to peak sooner than the less energetic x-ray emission. In examining the acceleration model in Figure 18, two explanations for the rise time of the soft x-ray bursts and the peak-to-peak delay time arise. The first of the two models makes two assumptions:

- (1) a significant part of the energy being carried into the soft x-ray flare region is in the form of the very energetic electrons which are also responsible for the microwave impulsive burst, and
- (2) the collisional thermalization time of the most energetic of these particles corresponds to the peak-to-peak delay time between the microwave and x-ray flare peaks.

The dominant feature of this model is that it does not necessarily require the acceleration mechanism to continue after time t_3 . It also assumes the electrons producing the microwave flare are crucial to the development of the soft x-ray flare.

The second model also makes two assumptions:

- (1) the thermalization time for all accelerated electrons is very short compared to the peak-to-peak time, and
- (2) the peak of the soft x-ray flare corresponds to the end of the acceleration mechanisms, that is, when no more energy is being deposited in the soft x-ray flare region.

Both models make assumptions regarding the collisional relaxation time in the flare region, so this is a logical point to pursue. The energy loss of an electron due to collisions is (Schatzman, 1965)

$$-\frac{d\epsilon}{dt} = \frac{\sqrt{2} A_a c}{\sqrt{\epsilon}}$$

where $\epsilon = T/m_0 c^2$ and A_a is roughly a constant given by

$$A_a = 1.14 \times 10^{-24} [2n_e (13.675 + \frac{1}{2} \log T/n_e + \log E) + n_0 (4.837 + \log E)]$$

where n_0 is the ion density. Integration of the above equation gives

$$\tau_{\text{decay}} = \frac{\sqrt{2}}{3} \frac{\epsilon^{3/2}}{A_a c}$$

If we take

$$T = 10^7 \text{ K}$$

and

$$n_e = n_o = 10^{10} \text{ cm}^{-3}$$

we have

$$A_a \sim 2 \times 10^{-13} .$$

The decay time in seconds then becomes

$$\tau_{\text{decay}} = 78 \frac{\epsilon^{3/2}}{n_e}$$

where n_e is the electron density in units of 10^{10} cm^{-3} .

It is obvious from the above relation that the feasibility of model 1 is highly dependent on the electron density in the soft x-ray flare region. Values between 10^9 cm^{-3} and 10^{12} cm^{-3} may be seriously considered, with most probable values of 10^{10} cm^{-3} to 10^{11} cm^{-3} .

For electron densities of 10^{10} cm^{-3} the decay time of a 700 keV electron would be in the vicinity of 2 min, a value which corresponds to the most probable value of the peak-to-peak delay time found in the present investigation. If electron densities in soft x-ray flare regions are consistently in the vicinity of 10^{11} cm^{-3}

the collisional lifetime of a 700 keV electron is on the order of 10 sec, and this model cannot account for the observed delay time distribution. If, however, the electron densities in x-ray flare regions are on the order of 10^{10} cm^{-3} or less fluctuations in this value from flare to flare could produce the observed distribution of peak-to-peak delay times.

Now a test will be made of the second assumption of the first model, that is, that the very energetic electrons responsible for the microwave burst carry sufficient energy to provide the power for the soft x-ray flare.

A solar flare electron spectrum in the range E at the peak of the microwave impulsive burst has been shown consistent with a power law of the following form (Takakura, 1969b):

$$\frac{dN(E)}{dE} = cE^{-\gamma}$$

where γ is most commonly found to be in the range 3—5. If we assume the spectrum can be represented by the same c and γ at all energies greater than 10 keV it is possible to calculate the energy contained in the energetic electron ensemble. The first step is to evaluate the constant c . The number of electrons of energy greater than 100 keV at the peak of the flash phase of the flare has been found to be (Holt and Ramaty, 1969) in the range 1.8×10^{35} to 8×10^{36} . This number shall be denoted by $N_{>100}$. It is obvious that

$$N_{>100} = \int_{100}^{\infty} c E^{-\gamma} dE ,$$

$$N_{>100} = \frac{c}{(\gamma - 1) 100^{(\gamma-1)}} .$$

$$\therefore c = (\gamma - 1) 100^{(\gamma-1)} N_{>100} .$$

The energy contained in the ensemble of electrons of energy greater than 10 keV is

$$\begin{aligned} E_{>10} &= c \int_{10}^{\infty} E^{-\gamma} E dE \\ &= \frac{c}{(\gamma - 2) 10^{(\gamma-2)}} . \end{aligned}$$

If we assume $\gamma = 3$ and take $N_{>100} = 10^{36}$ we have the energy contained in the energetic electron ensemble:

$$E_{>10} = 2 \times 10^{39} \text{ keV}$$

$$= 3.2 \times 10^{30} \text{ erg} .$$

A calculation will now be made of the energy contained in a soft x-ray flare region. A typical soft x-ray flare region has a volume of approximately 10^{28} cm^3 , in which there are roughly 10^{10} electrons/ cm^3 at a temperature of approximately $20 \times 10^6 \text{ K}$. The total energy contained in this region is thus

$$E_{\text{flare}} = V \cdot n_e \cdot E_e .$$

For the electron energy E_e we use

$$E_e = \frac{3}{2} kT .$$

where

$$T = 2 \times 10^7 \text{ K} .$$

Therefore

$$E_e = 4.1 \text{ keV} .$$

The total energy in the flare region is therefore

$$E_{\text{flare}} = 6.7 \times 10^{28} \text{ erg} .$$

The result is that more than an order of magnitude more energy is contained in the energetic particles that produce the microwave burst than in the soft x-ray flare region at its maximum temperature. It therefore appears that the requirement of the first model above, that the energetic particles have energy on the order of, or greater than, the energy in the soft x-ray flare region, is easily satisfied. A substantial fraction of the energy contained in this energetic electron ensemble is in the very energetic electrons of $E_e > 100$ keV, which will have decay times on the order of the peak-to-peak delay times observed. If the power law distribution holds throughout the $E > 10$ keV region, the ratio of the energy in the $E_e > 100$ keV range to the energy in the $10 \text{ keV} < E_e < 100 \text{ keV}$ range may be easily calculated in the same manner as above. It is found that, for $\gamma = 3$,

$$\frac{E_{<100}}{E_{>100}} \sim 9$$

If the electron distribution were to peak at some energy greater than 10 keV, rather than following a strictly power law form all the way to 10 keV, this ratio would, of course, be lower, which would render the contribution of the highly energetic electrons even more important.

We next consider the second assumption of model 2, which is that the peak of the soft x-ray flare corresponds to the end of

electron acceleration, that is, when no more energy is being deposited in the soft x-ray flare region. If we make the assumption that the end of the short-duration microwave flare represents the end of electron acceleration, the time delay between the end of the microwave flare and the peak of the x-ray flare becomes a meaningful parameter. McKenzie (1972) noted there was a tendency for radio emission to end near or after the soft x-ray peak.

In this study we have considered this point in more detail, as it may reflect on the feasibility of the second acceleration model presented above. In Figure 19 we have plotted the delay time between the end of the microwave flare and the peak of the soft x-ray flare for all events for which this parameter could be calculated.

Although a considerable range of values are observed, the distribution shows a definite maximum in the range 0 to +2 min. This means the microwave flares tend to peak from 0 to 2 min before the peak of the soft x-ray flares. This phenomenon is consistent with what would be expected if model 2 were indeed the operative mechanism. However, the existence of a large number (34%) with negative delay times, corresponding to the soft x-ray peak occurring before the end of the microwave flare, is inexplicable in terms of the simple model 2 advanced above. The observed large number of cases with negative delay times may be due to one or more of the following causes:

- (1) Characteristics of the electron acceleration mechanism in the electron energy range $E_e < E_s$ may be such as to produce the

soft x-ray peak while high energy electron acceleration was still taking place. We saw above that for $\gamma = 3$, the ratio of the energy in the electrons of energy less than 100 keV was 9 times that of the electrons of energy greater than 100 keV. If the power law index was larger, say 4 or 5, this ratio would be ever greater. One then might expect the peak of the soft x-ray flux to be determined by the ensemble of electrons of $E_e < 100$ keV. The microwave flares give no information about the behavior of the electron acceleration mechanism in the range $E_e < E_s$.

- (2) Cooling and expansion of the soft x-ray flare region may cause the time of peak x-ray emission to be different from the time expected from the simple model presented above.
- (3) Model 2 may simply be invalid, at least for those events with the time delay less than zero.

2. Flux and Energy Relationships

We now briefly review the findings of this study with regard to relationships between microwave and x-ray peak fluxes and the microwave and x-ray total energies.

This study found (Figure 16) a weak positive correlation between the microwave and x-ray flux changes in the sense that large amplitude microwave bursts tended to be accompanied by large amplitude x-ray events. It was noted, however, that there was a large dispersion in this relationship. Teske and Thomas (1969) found a

similar weak relationship. Culhane and Phillips (1970) found no such relationship, but the number of cases was too small to warrant a definite pronouncement.

The comparison between total soft x-ray energy and total microwave energy released during the duration of the respective events has been first attempted in this study. Arnoldy et al. (1968) compared the total energy released in associated microwave bursts and hard x-ray bursts. A positive correlation was found. The reason for the weakness of the flux-flux relationship and the absence of the energy-energy relationship in this study can be due to a number of causes:

- (1) the optical thickness due to gyro-synchrotron self absorption could vary from event to event, effecting both the microwave peak flux and total energy;
- (2) if the hard x-ray and microwave radiation originate from different flare regions than the soft x-ray burst, the ratio of the volumes of these regions, and hence the ratio of the number of emitters, could vary from event to event; and
- (3) the escape efficiency, or the number of particles which escape from the flare region before thermalizing, could vary from event to event. These particles could contribute to the microwave emission, but not to the heating of the x-ray region.

In summary, it has been seen that the first flare acceleration mechanism (no electron injection after the time corresponding to the

impulsive microwave burst peak) is in qualitative agreement with the observed delay time characteristics if the electron density in the soft x-ray flare is on the order of 10^{10} cm^{-3} . Additional assumptions must be made to account for the weakness of correlation between the microwave and x-ray peak fluxes and total energies.

If the soft x-ray flare electron densities are closer to 10^{11} cm^{-3} the second model (continued particle acceleration until at least the end of the short-duration microwave burst) is required to account for the observed peak-to-peak delay times. This model would make no predictions concerning amplitude or energy relationships due to the fact that the short-duration microwave burst gives no information about acceleration of electrons to energies less than E_s .

As stated previously, the most sensitive discrimination between these models relies upon more definite measurements of the electron densities in soft x-ray flares.

VII. CONCLUSIONS

The conclusions of this thesis are as follows:

- (1) Approximately 66% of all short-duration microwave bursts have associated soft x-ray events.
- (2) There is no evidence for the existence of subclasses of short-duration microwave bursts which originate from distinctly different physical mechanisms.
- (3) For 61% of the events observed, the defined start times of the microwave and x-ray bursts were within 2 min of each other, and 32% of the events had onsets that were simultaneous, ± 0.5 min. The manner in which the soft x-ray start time was defined would imply that, in general, x-ray activity preceded the microwave flare onset.
- (4) For 80% of the cases observed, the microwave flare reached maximum intensity from 0 to 7 min before the soft x-ray flare peak, with a most probable time delay of 2 ± 0.5 min.
- (5) A weak (0.43) but statistically significant relationship is found between the microwave and soft x-ray flux changes. The form of the relationship is similar to the relationship found by Teske and Thomas (1969).
- (6) A very weak (0.15) and statistically uncertain relationship was found between the total energy released by the microwave flare and the total energy released by the x-ray flare.

- (7) The observed peak-to-peak delay times are compatible with an impulsive electron acceleration mechanism if electron densities in the soft x-ray flare region are of the order of 10^{10} cm^{-3} , but a continuous acceleration mechanism is required if the electron densities in soft x-ray flare regions are of the order of 10^{11} cm^{-3} or higher.

ACKNOWLEDGMENTS

The author wishes to thank Dr. Stanley Shawhan for his advice and direction during the course of this project, and for his many valuable suggestions concerning the writing of this thesis.

Dr. James A. Van Allen is thanked for making available the Explorer 33 and 35 soft x-ray data.

I wish to express my appreciation to Dr. John D. Fix, who made a number of very helpful suggestions which rendered some points of the thesis more cogent and exact.

I greatly appreciate the help of Emmanuel T. Sarris, who shared with me his extensive knowledge of the subject of solar physics, and with whom I had many very informative discussions.

Thanks are due to Davis D. Sentman for help in computer programming and for many discussions on the topic.

I wish to acknowledge the help of many members of the staff of the Department of Physics and Astronomy. Angie McAllister is thanked for punching the computer cards on which the data used in this study are recorded. The conversion from cryptic scratchings to typed copy was accomplished by Shirley Streeby, and is sincerely appreciated. David D. Dunlavy is thanked for operation of the North Liberty Radio Observatory during the time data was being taken. The plots for this thesis were done by John Birkbeck and Joyce Chrisinger,

and their help is gratefully acknowledged. Finally, the help of Mike Williams is greatly appreciated for assistance in operation of the Univac 418 computer on which data analysis was carried out. I thank him for always being conveniently near when the machine "mysteriously" shut itself off.

Finally, I wish to thank my wife Carol for support and encouragement during the course of this work.

Support for this thesis has been provided by the Office of Naval Research through contract N00014-68-A-0196-0003 and the National Aeronautics and Space Administration through grant NGL-16-001-002.

Table 2

Comparison between NLRO and Sagamore Hill
flux values for several selected events.

Date	Time (UT)	Flux Change [Solar Flux Units]	
		NLRO	Sagamore Hill [*]
Feb. 7, 1969	1645	132 ± 11	84.0
Feb. 8, 1969	1751	83 ± 6	52.0
May 22, 1969	1935	396 ± 41	255.0
July 3, 1969	1518	272 ± 5	225.0
Aug. 12, 1969	1555	71 ± 13	47.0

* All Sagamore Hill flux values have uncertainties of 5—10%.

E

Table 3

List of 259 microwave flares and
associated soft x-ray emission.

A. Microwave flares observed at NLRO

	Date	Start	Peak	End	Flux Change
01	11-03-68	1641.0	1642.0	1643.0	127+.7
01	11-25-68	1632.0	1632.8	1633.1	137+43
01	11-27-68	1822.5	1823.0	1824.0	52+1.4
01	12-12-68	1534.0	1543.2	1535.4	132+41
01	12-20-68	2012.0	2016.0	2020.0	
01	12-24-68	1702.1	1702.3	1702.7	99+14
01	12-26-68	2022.0	2023.1	2025.0	224+62
01	01-04-69	2059.0	2103.0	2106.0	99+43
01	01-05-69	1631.0	1631.0	1631.5	84+36
01	02-01-69	1502.5	1503.0	1503.5	61+19
01	02-01-69	1505.0	1509.0	1515.0	89+28
01	02-02-69	2103.5	2106.3	2107.0	123+82
01	02-03-69	2133.0	2135.1	2135.8	40+12
01	02-07-69	1645.0	1645.5	1647.0	132+11
01	02-08-69	1750.5	1751.0	1752.0	83+6
01	02-08-69	1755.0	1756.0	1757.0	77+6
01	02-14-69	1909.0	1909.2	1909.5	68+28
01	02-14-69	1909.5	1910.0	1910.5	68+28
01	02-14-69	1913.0	1913.5	1914.0	68+28
01	02-15-69	1829.0	1830.0	1830.7	48+10
01	02-15-69	2113.2	2113.7	2114.0	39+17
01	02-15-69	2118.3	2118.7	2119.0	47+21
01	02-17-69	1809.0	1809.5	1810.0	54+4
01	02-17-69	2019.0	2019.7	2020.5	68+21
01	02-18-69	1850.0	1851.0	1852.0	44+12
01	02-19-69	1936.0	1937.2	1939.0	197+72
01	02-19-69	1601.2	1601.5	1601.6	75+24
01	02-24-69	1737.5	1738.0	1739.0	63+7
01	02-24-69	2312.0	2316.0	2322.0	560+42
01	02-25-69	1656.6	1658.9	1705.0	728+26
01	02-25-69	1939.0	1942.0	1945.0	133+45
01	02-26-69	1713.0	1713.5	1714.0	80+27
01	02-26-69	1716.0	1716.5	1717.0	78+26

Table 3 (continued)

A. (continued)

	Date	Start	Peak	End	Flux Change
01	03-21-69	1537.5	1538.0	1538.5	1353+392
01	03-21-69	1343.0	1344.0	1348.0	405+.6
01	03-23-69	1824.0	1824.2	1825.0	120+15
01	05-22-69	1932.0	1935.1	1937.5	396+41
01	07-03-69	1517.0	1518.0	1520.0	272+.5
01	08-12-69	1555.0	1555.5	1557.0	71+13
01	08-14-69	1546.8	1547.0	1548.0	86+23
01	08-15-69	2235.7	2236.0	2236.1	58+10
01	08-15-69	2238.8	2239.0	2239.0	58+10
01	09-14-69	2301.0	2301.5	2302.5	393+38
01	11-05-69	1759.0	1801.0	1802.5	98+21
01	11-18-69	2029.0	2029.5	2030.0	96+20
01	11-18-69	2121.9	2123.0	2124.2	2399+.8
01	11-19-69	1707.0	1707.2	1707.8	164+.7
01	11-20-69	2144.2	2144.9	2145.0	154+48
01	11-20-69	2031.0	2031.5	2032.0	140+32
01	11-21-69	1727.7	1728.0	1731.0	167+2.7
01	11-28-69	1930.0	1932.6	1941.0	5730+1097
01	11-28-69	2134.8	2135.7	2137.5	85+24
01	11-30-69	1706.0	1707.0	1708.0	71+22
01	03-08-70	2104.0	2104.5	2105.0	
01	03-17-70	1753.5	1754.5	1755.0	

Table 3 (continued)

B. Soft x-ray emission associated with
radio bursts observed at NLRO.

	Date	Start	Peak	End	SUMF	Δs
02	11-02-68	1510.0	1544.0	1552.0	0.825	7.0
02	11-03-68	1639.0	1643.0	1652.0	1.269	2.7
02	11-25-68		NO	FLARE		
02	11-27-68	1814.0	1828.0	1959.0	0.853	0.36
02	12-12-68	1531.0	1538.0	1610.0	0.599	0.6
02	12-20-68	1939.0	1959.0	2111.0	42.114	20.9
02	12-24-68		DATA	GAP		
02	12-26-68	2014.0	2020.0	2040.0		
02	01-04-69	2100.0	2114.0	2148.0	98.427	61.3
02	01-05-69	1537.0	1556.0	1703.0	5.288	2.6
02	02-01-69		NO	FLARE		
02	02-01-69		NO	FLARE		
02	02-02-69		NO	FLARE		
02	02-03-69	2126.0	2133.0	2145.0	1.174	2.14
02	02-07-69	1645.0	1647.0	1654.0	3.653	9.6
02	02-08-69	1713.0	1755.0	1809.0	1.772	17.2
02	02-08-69	1750.0	1755.0	1809.0	1.772	17.2
02	02-14-69		DATA	GAP		
02	02-14-69		DATA	GAP		
02	02-14-69		DATA	GAP		
02	02-15-69		NO	FLARE		
02	02-15-69	2016.0	2122.0	2230.0	3.191	0.67
02	02-15-69	2016.0	2122.0	2230.0	3.191	0.67
02	02-17-69		DATA	GAP		
02	02-17-69		DATA	GAP		
02	02-18-69		DATA	GAP		
02	02-19-69		NO	FLARE		
02	02-19-69	1600.0	1603.0	1607.0	0.441	2.2
02	02-24-69		NO	FLARE		
02	02-24-69	2313.0	2322.0	0005.0	125.628	80.5
02	02-25-69	1642.0	1712.0	1749.0	12.960	5.0
02	02-25-69	1941.0	1955.0	2045.0	40.990	27.1
02	02-26-69		NO	FLARE		
02	02-26-69		NO	FLARE		
02	03-21-69	1539.5	1543.0	1613.0	8.884	126.0
02	03-21-69	1308.0	1346.0	1540.0	300.070	126.0
02	03-23-69	1813.0	1824.0	1846.0	6.948	8.8

Table 3 (continued)

B. (continued)

	Date	Start	Peak	End	SUMF	Δs
02	05-22-69	1902.0	1908.0	2002.0	21.945	36.0
02	07-03-69	1517.0	1525.0	1540.0	60.134	42.8
02	08-12-69	1552.0	1555.0	1621.0	5.256	1.44
02	08-14-69		NO	FLARE		
02	08-15-69		FLARE OCCURS, BREAK IN DATA			
02	09-14-69	2251.0	2309.0	2323.0	0.319	0.5
02	11-05-69	1753.0	1805.0	1823.0	10.867	15.7
02	11-18-69		DATA	GAP		
02	11-18-69	2117.0	2125.0	2142.0		
02	11-19-69	1630.0	1658.0	1900.0	310.667	8.8
02	11-20-69	2122.0	2134.0	2202.0	0.719	1.25
02	11-20-69		FLARE EXISTS, BREAK IN DATA			
02	11-21-69	1716.0	1729.0	1754.0	3.890	5.0
02	11-28-69	1917.0	2047.0	2330.0	618.021	138.0
02	11-28-69	1917.0	2047.0	2330.0	618.021	138.0
02	11-30-69	1703.0	1710.0	1750.0	2.287	2.16
02	03-08-70		DATA	GAP		
02	03-17-70		DATA	GAP		

Table 3 (continued)

C. Microwave flares observed at Sagamore Hill.

	Date	Start	Peak	Dur.	Δs_{\max}	Δs_{mean}	Class
03	01-04-68	1326.0	1326.3	3.2	138.5	62.5	3
03	01-04-68	1657.3	1657.8	0.9	23.1	10.4	3
03	01-04-68	1752.5	1752.6	1.8	11.5	5.2	3
03	01-05-68	1225.2	1225.4	0.8	91.8	22.4	3
03	01-06-68	1953.1	1953.5	3.6	11.6	6.9	1
03	01-07-68	1740.7	1740.7	1.3	17.5	1.2	3
03	01-08-68	1509.8	1509.9	0.7	23.5	13.5	3
03	01-10-68	1442.0	1442.6	2.5	6.0	2.0	1
03	01-12-68	1809.5	1809.8	1.5	108.0	21.0	3
03	01-13-68	1240.5	1240.6	2.5	28.0	11.0	3
03	01-13-68	1454.2	1457.3	6.4	6.0	3.0	1
03	01-13-68	1848.6	1850.8	5.8	11.0	4.0	3
03	01-14-68	1840.3	1841.2	6.6	63.0	16.0	3
03	01-15-68	1434.3	1434.7	3.2	12.0	6.0	3
03	01-15-68	1745.7	1745.9	1.1	9.0	3.0	1
03	01-26-68	1413.5	1415.8	6.1	18.0	4.0	3
03	01-27-68	1221.5	1221.7	0.5	25.0	12.0	3
03	01-29-68	1538.6	1539.3	8.9	165.0	41.0	3
03	01-29-68	2009.8	2010.0	2.2	36.0	18.0	3
03	01-30-68	1510.6	1511.4	3.5	110.0	20.0	3
03	01-30-68	2014.8	2016.1	2.6	57.0	38.0	3
03	01-31-68	1341.2	1342.7	4.8	11.0	4.0	3
03	02-01-68	1610.2	1610.3	1.4	57.0	28.0	3
03	02-01-68	1802.2	1802.7	3.0	840.0	280.0	3
03	02-02-68	1428.6	1428.8	1.2	3.0	1.5	1
03	02-03-68	1335.8	1337.8	7.2	165.0	62.0	3
03	02-10-68	1914.7	1915.7	3.4	140.0	5.0	3
03	02-14-68	1534.5	1535.4	5.3	59.0	21.0	3
03	02-16-68	1602.7	1603.5	3.5	46.0	28.0	3
03	02-17-68	1255.7	1256.3	1.7	47.4	24.3	3
03	03-12-68	2105.0	2107.7	4.8	15.6	8.0	3
03	03-21-68	1914.6	1915.4	1.8	4.0	2.0	1
03	04-01-68	1307.2	1308.1	6.3	5.3	1.8	1
03	04-02-68	1614.8	1615.3	4.1	5.1	2.5	1
03	04-03-68	2210.7	2210.0	0.6	9.2	4.5	3
03	04-12-68	1252.2	1252.6	0.9	4.0	2.0	1
03	04-14-68	1204.5	1204.8	1.0	9.2	4.7	3
03	04-19-68	1609.0	1610.4	3.5	6.0	2.5	1

Table 3 (continued)

C. (continued)

	Date	Start	Peak	Dur.	Δs_{\max}	Δs_{mean}	Class
03	04-25-68	1255.6	1257.3	2.3	3.5	1.8	1
03	04-29-68	1134.4	1134.6	1.4	8.6	3.2	3
03	05-03-68	1209.7	1209.9	0.5	4.2	2.0	1
03	05-03-68	1659.8	1700.2	2.4	2.9	1.0	1
03	05-03-68	2225.8	2226.1	0.9	8.4	2.4	3
03	05-05-68	1408.4	1408.7	1.1	3.8	1.4	1
03	05-08-68	1234.3	1234.4	0.5	9.4	3.1	3
03	05-08-68	1416.3	1417.7	2.8	5.6	2.8	1
03	05-16-68	1034.0	1037.0	6.8	4.2	2.8	1
03	05-17-68	1606.1	1610.1	6.8	6.6	3.3	1
03	05-19-68	1227.9	1228.4	4.4	5.9	2.8	1
03	05-19-68	1412.4	1413.2	2.6	2.9	1.2	1
03	05-20-68	1857.7	1857.8	0.3	16.8	7.0	3
03	05-22-68	1827.9	1828.5	1.2	23.5	9.2	3
03	05-24-68	1716.2	1716.9	3.0	14.2	4.6	3
03	05-24-68	1825.1	1826.2	2.0	18.9	6.3	3
03	05-25-68	1956.0	1956.6	5.1	11.8	5.0	3
03	05-26-68	2021.4	2022.0	5.6	9.7	4.0	3
03	06-11-68	2046.1	2046.3	1.9	7.6	1.8	3
03	06-12-68	1647.0	1647.7	3.0	39.1	13.3	3
03	06-13-68	2133.3	2133.7	5.6	7.6	2.5	3
03	06-19-68	1740.0	1740.3	1.0	7.4	5.0	1
03	06-19-68	2224.7	2225.2	7.5	19.6	6.5	3
03	06-21-68	1024.2	1025.4	2.4	11.9	7.2	3
03	06-22-68	1715.9	1716.1	0.4	5.5	2.1	1
03	06-24-68	1137.0	1137.3	1.1	8.4	4.2	3
03	06-27-68	1939.0	1941.4	5.8	10.1	4.0	3
03	06-30-68	1432.2	1432.7	1.2	3.8	1.9	1
03	07-03-68	2328.8	2329.3	2.6	32.6	7.5	3
03	07-05-68	2245.7	2246.7	1.9	7.9	3.0	3
03	07-06-68	1453.3	1453.4	1.6	3.7	1.6	1
03	07-06-68	1552.1	1552.2	6.0	88.8	21.4	3
03	07-10-68	2231.4	2235.1	6.1	15.2	5.0	3
03	07-11-68	1126.9	1130.0	7.8	1.9	1.0	20
03	07-13-68	1350.4	1350.9	1.3	3.9	1.8	1
03	07-13-68	1451.6	1452.2	1.6	4.3	2.0	1
03	07-14-68	1030.2	1031.3	3.2	14.5	.3	3
03	07-14-68	1441.0	1441.3	0.9	4.7	2.3	1

Table 3 (continued)

C. (continued)

	Date	Start	Peak	Dur.	Δs_{\max}	Δs_{mean}	Class
03	07-26-68	1232.0	1233.3	2.8	14.8	6.1	3
03	07-26-68	1245.0	1245.4	1.0	5.6	2.8	1
03	07-30-68	2029.5	2031.1	4.5	30.8	15.4	3
03	08-05-68	1838.1	1838.3	0.9	8.2	4.1	3
03	08-05-68	2054.2	2054.7	5.0	13.5	6.0	3
03	08-12-68	1056.0	1056.3	0.6	11.2	5.6	3
03	08-12-68	1153.7	1154.2	1.6	29.2	9.7	3
03	08-13-68	1254.2	1254.8	9.0	125.0	40.5	3
03	08-15-68	1141.4	1146.5	7.9	5.4	2.5	20
03	08-22-68	1554.4	1555.0	1.4	5.9	4.0	1
03	08-23-68	1459.8	1500.0	0.5	17.2	8.6	3
03	09-09-68	1747.5	1748.2	1.6	6.2	3.1	1
03	09-10-68	2012.4	2012.7	5.8	24.0	8.0	3
03	09-28-68	1742.2	1742.6	3.3	9.5	4.6	3
03	10-12-68	2005.1	2005.5	0.8	9.2	4.0	3
03	10-17-68	1257.0	1257.7	2.3	4.3	2.2	1
03	10-17-68	2130.4	2130.6	2.3	11.0	3.7	3
03	10-19-68	1852.3	1852.5	0.4	7.0	3.5	1
03	10-20-68	1928.8	1930.2	7.2	18.9	5.0	3
03	10-21-68	1425.6	1426.1	0.8	10.2	5.1	3
03	10-23-68	1740.7	1741.8	7.9	8.2	4.0	20
03	11-01-68	1304.3	1305.3	2.7	4.9	2.0	1
03	11-01-68	1331.2	1331.9	2.8	4.9	2.0	1
03	11-01-68	1713.9	1714.0	2.1	27.4	6.0	3
03	11-01-68	1930.2	1930.3	1.3	5.1	1.7	1
03	11-02-68	1912.0	1913.5	4.5	18.9	9.4	3
03	11-03-68	1809.9	1810.5	1.4	5.5	2.8	1
03	11-03-68	1933.9	1934.3	1.3	11.0	3.7	3
03	11-05-68	1238.2	1238.3	0.3	5.0	2.5	1
03	11-05-68	1342.3	1343.3	3.2	33.2	8.0	3
03	11-06-68	1226.2	1226.8	1.0	43.4	22.0	3
03	11-06-68	1302.5	1302.8	1.3	6.1	3.3	1
03	11-11-68	1442.1	1444.0	6.2	5.4	2.7	1
03	11-11-68	1555.2	1555.4	1.4	1.6	0.8	1
03	11-11-68	1626.1	1626.3	0.4	21.6	10.8	3
03	11-11-68	2014.9	2015.0	0.9	5.4	2.7	1
03	11-12-68	1725.4	1725.9	1.4	59.0	19.5	3
03	11-13-68	1414.2	1414.3	0.8	3.1	1.5	1
03	11-15-68	1659.4	1659.5	0.7	16.2	8.0	3

Table 3 (continued)

C. (continued)

	Date	Start	Peak	Dur.	Δs_{\max}	Δs_{mean}	Class
03	11-17-68	1657.6	1657.8	4.0	5.9	2.5	1
03	11-18-68	1501.0	1504.0	7.1	14.3	5.8	3
03	11-22-68	1321.4	1321.9	5.9	225.0	45.0	3
03	11-27-68	1822.6	1823.1	3.8	36.2	8.1	3
03	12-08-68	1523.4	1524.3	9.7	12.1	5.5	3
03	12-12-68	1812.0	1812.2	0.8	7.2	3.6	1
03	12-20-68	1940.1	1943.2	6.5	22.0	11.0	3
03	12-21-68	1814.6	1815.1	1.4	5.0	2.5	1
03	12-22-68	1604.6	1604.7	0.9	4.5	2.0	1
03	12-22-68	1830.8	1831.1	5.4	14.0	6.0	3
03	12-23-68	1513.2	1513.3	1.5	9.3	4.0	3
03	12-26-68	1554.5	1555.2	1.8	3.6	1.5	1
03	12-26-68	1903.2	1904.0	1.2	2.6	1.0	1
03	12-29-68	1406.6	1406.9	0.6	13.0	7.4	3
03	12-29-68	1428.1	1428.7	1.6	57.7	38.4	3
03	12-29-68	1827.6	1829.0	4.7	17.1	8.6	3
03	12-30-68	1437.8	1438.1	2.4	29.2	11.0	3
03	12-30-68	1637.5	1637.8	8.7	34.0	8.1	3
03	01-08-69	2037.4	2037.8	2.4	29.4	5.0	3
03	01-09-69	1831.6	1835.8	5.5	32.2	21.4	3
03	01-09-69	2012.3	2015.0	5.0	15.6	7.8	3
03	01-16-69	1323.6	1323.8	0.7	5.0	2.0	1
03	01-21-69	1250.8	1252.0	3.6	22.4	10.2	3
03	01-25-69	1409.4	1409.6	0.4	7.1	3.5	1
03	02-07-69	1644.8	1645.5	2.0	84.0	10.3	3
03	02-13-69	1637.0	1637.1	1.1	8.4	4.2	3
03	02-22-69	1734.6	1737.4	5.4	7.4	3.7	1
03	02-22-69	1922.0	1922.4	4.6	6.3	3.2	1
03	02-24-69	1504.3	1505.9	2.4	7.6	3.0	3
03	02-24-69	1737.4	1737.7	1.5	19.3	13.6	3
03	02-28-69	1340.4	1340.8	3.8	62.0	12.0	3
03	03-08-69	1438.3	1438.7	2.5	14.4	4.0	3
03	03-09-69	1816.5	1817.0	3.9	4.4	1.5	1
03	03-09-69	1916.7	1920.7	7.0	8.0	2.0	20
03	03-12-69	2010.1	2010.4	1.9	15.1	7.5	3
03	03-13-69	1316.8	1317.8	2.2	3.4	1.5	1
03	03-13-69	1705.0	1707.0	3.8	12.9	3.0	3
03	03-17-69	1247.1	1247.3	0.8	4.4	2.0	1
03	03-17-69	1919.3	1919.8	5.7	11.3	3.0	3

Table 3 (continued)

C. (continued)

	Date	Start	Peak	Dur.	Δs_{\max}	Δs_{mean}	Class
03	03-18-69	1155.6	1155.9	0.7	3.6	1.8	1
03	03-19-69	1858.9	1859.0	5.1	13.6	3.2	3
03	03-20-69	1446.9	1447.0	0.3	2.8	1.4	1
03	03-20-69	1754.0	1754.4	3.0	4.6	2.0	1
03	03-21-69	1306.0	1309.6	7.8	9.4	3.2	20
03	03-22-69	1211.6	1212.8	0.9	92.0	23.0	3
03	03-23-69	1924.2	1924.4	2.6	70.0	28.0	3
03	03-23-69	2040.4	2041.2	2.6	5.4	2.7	1
03	03-26-69	1640.7	1641.0	0.9	4.3	2.2	1
03	03-26-69	1856.7	1857.0	4.0	100.0	21.0	3
03	04-01-69	1142.2	1143.0	8.8	8.8	4.2	3
03	04-01-69	1331.6	1332.4	2.4	4.2	2.1	1
03	04-01-69	2202.0	2202.4	1.0	8.6	3.0	3
03	04-04-69	1712.4	1713.0	2.9	8.4	3.4	3
03	04-14-69	1930.0	1934.4	8.8	4.3	2.1	20
03	04-15-69	1156.0	1159.9	8.0	5.0	2.0	20
03	04-21-69	1220.5	1221.1	1.2	9.7	3.0	3
03	04-24-69	1245.4	1246.0	6.6	8.8	4.3	3
03	04-26-69	1502.1	1502.9	3.9	4.5	3.0	1
03	05-02-69	2105.2	2105.3	3.0	25.9	12.9	3
03	05-04-69	2050.0	2050.5	2.0	5.8	2.8	1
03	05-18-69	1718.6	1718.9	1.2	61.0	18.8	3
03	05-18-69	2107.2	2107.3	0.8	15.0	17.1	3
03	05-20-69	1218.0	1218.4	1.2	4.8	2.0	1
03	05-28-69	1440.4	1442.0	6.1	3.8	1.9	1
03	05-29-69	1718.5	1719.1	3.0	18.5	9.2	3
03	06-05-69	2134.7	2135.5	1.4	15.3	7.5	3
03	06-06-69	1037.8	1038.3	6.7	6.2	2.4	1
03	06-06-69	1604.1	1606.5	8.9	15.6	8.0	3
03	06-06-69	1953.5	1954.0	0.8	10.6	5.0	3
03	06-09-69	1035.0	1035.3	1.3	6.5	3.2	1
03	06-09-69	1205.9	1206.2	2.4	7.6	3.8	3
03	06-09-69	1850.6	1851.1	5.4	24.9	10.2	3
03	06-09-69	2047.3	2048.4	3.9	7.0	3.5	1
03	06-09-69	2153.5	2154.0	3.6	10.8	5.4	3
03	06-09-69	2249.6	2251.5	3.4	17.2	8.0	3
03	06-10-69	1551.0	1551.4	1.3	5.4	2.4	1
03	06-10-69	1710.0	1710.6	1.6	12.9	6.4	3

Table 3 (continued)

C. (continued)

	Date	Start	Peak	Dur.	Δs_{\max}	Δs_{mean}	Class
03	06-11-69	1207.0	1207.3	1.0	7.6	3.8	3
03	06-12-69	1101.3	1101.5	0.8	11.0	5.5	3
03	06-14-69	2017.2	2017.4	0.4	18.2	9.1	3
03	06-16-69	2021.4	2021.7	1.6	17.1	8.6	3
03	06-18-69	1526.6	1526.7	0.7	8.6	4.3	3
03	06-18-69	2251.1	2251.4	0.9	8.9	4.5	3
03	07-05-69	1847.6	1848.8	8.4	11.2	4.0	20
03	07-05-69	1958.0	1959.3	2.0	6.6	3.0	1
03	07-14-69	1431.2	1431.6	2.1	18.5	6.9	3
03	07-31-69	1029.1	1029.4	0.8	8.4	4.0	3
03	08-01-69	2153.9	2154.4	1.3	5.3	2.6	1
03	08-10-69	1422.6	1423.2	1.3	21.0	10.4	3
03	08-11-69	1219.8	1220.0	3.2	23.0	8.8	3
03	08-11-69	1649.3	1649.7	1.0	19.7	4.0	3
03	08-12-69	1555.2	1555.7	1.8	47.0	14.0	3

Table 3 (continued)

D. Soft x-ray emission associated with radio
bursts observed at Sagamore.

	Date	Start	Peak	End	SUMF	Δs
04	01-04-68	1321.40	1338.52	1405.27	3.720	2.38
04	01-04-68		DATA	GAP		
04	01-04-68		1753.50	1758.38	3.590	16.6
04	01-05-68	1225.6	1227.47	1233.52	8480	81
04	01-06-68		NO	FLARE		
04	01-07-68		NO	FLARE		
04	01-08-68		NO	FLARE		
04	01-10-68		DATA	GAP		
04	01-12-68	1809.14	1812.43	1823.09	14.161	27.3
04	01-13-68		DATA	GAP		
04	01-13-68	1452.10	1454.49	1458.38	1.715	7.0
04	01-13-68	1845.15	1849.20	1853.46	2.339	8.2
04	01-14-68	1839.44	1847.46	1904.54	3.628	4.3
04	01-15-68	1420.21	1503.58	1627.47	11.466	2.0
04	01-15-68		NO	FLARE		
04	01-26-68	1412.56	1414.08	1418.10	0.588	3.3
04	01-27-68	1201.48	1226.14	1244.56	1.188	1.53
04	01-29-68	1539.19	1544.47			37.5
04	01-29-68	2003.31	2010.47	2013.15	0.498	2.8
04	01-30-68	1512.10	1516.50			6.3
04	01-30-68	2014.26	2021.30	2114.28	18.780	12.0
04	01-31-68		NO	FLARE		
04	02-01-68		NO	FLARE		
04	02-01-68	1759.52	1806.08	1826.54	23.070	22.0
04	02-02-68		NO	FLARE		
04	02-03-68	1336.00	1342.36	1354.00	14.468	19.5
04	02-10-68	1905.44	1928.50	2131.50	9.755	39.0
04	02-14-68	1534.52	1536.14			11.3
04	02-16-68	1603.25	1607.18	1615.03	4.694	11.7
04	02-17-68	1256.05	1258.48			15.7
04	03-12-68	2107.03	2109.10	2112.42	0.349	2.0
04	03-21-68	1912.51	1916.56	1923.37	16.765	54.0
04	04-01-68	1303.55	1309.22	1314.31	1.556	5.5
04	04-02-68		DATA	GAP		
04	04-03-68	2206.16	2214.21	2236.58	0.864	0.9

Table 3 (continued)

D. (continued)

	Date	Start	Peak	End	SUMF	Δs
04	04-12-68		NO	FLARE		
04	04-14-68		NO	FLARE		
04	04-19-68	1610.30	1615.44	1626.38	0.754	1.4
04	04-25-68	FLARE OCCURS, DATA INSUFFICIENT FOR PARAMETERS				
04	04-29-68	1056.40	1124.40	1142.58	4.782	3.2
04	05-03-68	1053.42	1212.57	1312.55	4.736	1.5
04	05-03-68		NO	FLARE		
04	05-03-68		DATA	GAP		
04	05-05-68	1406.90	1409.48	1415.32	1.005	2.8
04	05-08-68		NO	FLARE		
04	05-08-68		NO	FLARE		
04	05-16-68	1036.21	1047.70	1100.36	4.759	4.2
04	05-17-68	1606.20	1612.48	1658.31	2.301	1.9
04	05-19-68	1225.36	1237.19	1251.12	1.017	1.9
04	05-19-68	1412.25	1415.70	1427.70	1.174	2.5
04	05-20-68		NO	FLARE		
04	05-22-68	1828.13	1830.51	1401.22	5.017	5.4
04	05-24-68		NO	FLARE		
04	05-24-68		NO	FLARE		
04	05-25-68		NO	FLARE		
04	05-26-68		NO	FLARE		
04	06-11-68		NO	FLARE		
04	06-12-68	1647.23	1651.60	1705.60	1.182	2.2
04	06-13-68	2133.70	2134.29	2144.26	0.766	2.2
04	06-19-68		DATA	GAP		
04	06-19-68	2226.37	2230.31	2256.51	18.740	18.0
04	06-21-68		DATA	GAP		
04	06-22-68	1647.41	1702.40	1724.16	1.351	1.2
04	06-24-68		1139.70	1216.35	11.750	1.6
04	06-27-68	1940.56	1953.27	2037.29	5.050	3.3
04	06-30-68		NO	FLARE		
04	07-03-68	FLARE EXISTS, DATA DISCONTINUITIES				
04	07-05-68		2249.20	2353.57	36.090	7.2
04	07-06-68		NO	FLARE		
04	07-06-68	1551.45	1554.21	1605.55	2.623	5.4
04	07-10-68		NO	FLARE		
04	07-11-68	0758.38	1136.59	1303.58	44.491	3.9
04	07-13-68	1321.50	1402.34	1626.19	52.650	0.5
04	07-13-68	1451.60	1455.37	1521.26	2.829	2.5

Table 3 (continued)

D. (continued)

	Date	Start	Peak	End	SUMF	As
04	07-14-68	1029.41	1032.17	1054.13	2.775	3.5
04	07-14-68	1436.30	1502.14	1647.13	6.524	1.2
04	07-26-68	1232.53	1235.13	1237.53	0.257	1.3
04	07-26-68		DATA	GAP		
04	07-30-68	2029.38	2032.22			12.5
04	08-05-68	1827.27	1842.37	1911.50	1.765	1.8
04	08-05-68	2054.80	2101.42	2116.80	1.314	1.3
04	08-12-68	1038.32	1057.36	1115.70	1.315	1.0
04	08-12-68		NO	FLARE		
04	08-13-68	1250.50	1256.10	1302.20	3.677	13.1
04	08-15-68	1140.26	1146.40	1209.39	1.019	1.6
04	08-22-68	1504.46	1613.13	1700.16	19.280	5.0
04	08-23-68	1459.30	1500.45	1504.90	2.554	21.0
04	09-09-68	1745.20	1750.26	1800.48	5.179	4.1
04	09-10-68	2012.59	2019.48			5.6
04	09-28-68	1741.58	1745.11	1750.37	0.479	1.8
04	10-12-68	2004.35	2007.10	2021.20	3.545	7.5
04	10-17-68	1246.30	1304.39	1319.40	3.109	3.0
04	10-17-68	2128.12	2131.51	2204.70	4.970	4.3
04	10-19-68	1851.56	1858.45			7.0
04	10-20-68	1803.19	1932.37	2024.49	23.672	8.1
04	10-21-68	1419.40	1433.49	1549.11	1.963	22.7
04	10-23-68	1741.43	1745.38	1804.80	1.184	5.0
04	11-01-68		NO	FLARE		
04	11-01-68		NO	FLARE		
04	11-01-68		NO	FLARE		
04	11-01-68		NO	FLARE		
04	11-02-68		NO	FLARE		
04	11-03-68	1809.11	1812.00	1817.53	0.717	2.3
04	11-03-68		NO	FLARE		
04	11-05-68		DATA	GAP		
04	11-05-68	1342.31	1345.43	1354.36	1.881	4.4
04	11-06-68		NO	FLARE		
04	11-06-68		NO	FLARE		
04	11-11-68	1442.10	1447.13	1509.13	2.103	2.8
04	11-11-68		DATA	GAP		

Table 3 (continued)

D. (continued)

	Date	Start	Peak	End	SUMF	Δs	
04	11-11-68		DATA	GAP			
04	11-11-68		NO	FLARE			
04	11-12-68	1725.32	1751.40	1830.70	4.330	1.9	
04	11-13-68		DATA	GAP			
04	11-15-68		NO	FLARE			
04	11-17-68	1657.29	1703.43	1729.36	3.817	3.4	
04	11-18-68		NO	FLARE			
04	11-23-68	1321.55	1324.21	1333.19	2.754	7.5	
04	11-27-68		DATA	GAP			
04	12-08-68	1523.33	1529.33	1551.12	5.268	5.2	
04	12-12-68		NO	FLARE			
04	12-20-68	1939.27	2000.00			14.6	
04	12-21-68	1741.55	1758.21	1853.90	5.233	2.2	
04	12-22-68		NO	FLARE			
04	12-22-68	1830.54	1853.37			2.4	
04	12-23-68	1512.18	1514.21	1519.29	0.271	1.1	
04	12-26-68		NO	FLARE			
04	12-26-68		DATA	GAP			
04	12-29-68		DATA	GAP			
04	12-29-68	1426.58	1435.10	1513.46	3.129	3.0	
04	12-29-68		DATA	GAP			
04	12-30-68		NO	FLARE			
04	12-30-68		DATA	GAP			
04	01-08-69	2037.27	2041.13	2109.18	4.447	5.1	
04	01-09-69	FLARE EXISTS, DATA DISCONTINUITY					
04	01-09-69		NO	FLARE			
04	01-16-69	1322.36	1326.50	1338.48	2.541	8.1	
04	01-21-69		NO	FLARE			
04	01-25-69	1409.21	1412.40	1439.38	11.066	14.0	
04	02-07-69	1645.30	1647.40	1654.56	3.653	9.3	
04	02-13-69	1632.19	1638.19	1649.40	3.945	7.0	
04	02-22-69		NO	FLARE			
04	02-22-69	1920.29	1927.00	1945.25	3.650	4.9	
04	02-24-69	1500.38	1508.55	1537.60	7.947	5.3	
04	02-24-69		NO	FLARE			
04	02-28-69	1339.14	1355.37	1422.56	1.130	12.9	
04	03-08-69		NO	FLARE			

F

Table 3 (continued)

D. (continued)

	Date	Start	Peak	End	SUMF	As
04	03-09-69		NO	FLARE		
04	03-09-69	1917.50	1922.40	1931.58	7.108	12.7
04	03-12-69	2002.59	2011.10	2047.10	4.648	28.6
04	03-13-69	1317.25	1323.18	1330.34	1.611	4.0
04	03-13-69	1707.57	1714.46			4.0
04	03-17-69		NO	FLARE		
04	03-17-69	1919.00	1921.50	2010.08	24.034	7.4
04	03-18-69	1155.23	1159.08	1236.22	3.742	10.0
04	03-19-69	1643.34	1901.37	2110.52	31.441	2.9
04	03-20-69		NO	FLARE		
04	03-20-69		NO	FLARE		
04	03-21-69		NO	FLARE		
04	03-22-69		NO	FLARE		
04	03-23-69		DATA	GAP		
04	03-23-69		NO	FLARE		
04	03-26-69		NO	FLARE		
04	03-26-69		DATA	GAP		
04	04-01-69		NO	FLARE		
04	04-01-69		DATA	GAP		
04	04-01-69		DATA	GAP		
04	04-04-69	1745.23	1747.55	1800.59	0.546	1.9
04	04-14-69	1928.37	1934.33	1951.00	6.036	7.6
04	04-15-69		DATA	GAP		
04	04-21-69	1220.57	1222.18	1233.36	2.541	4.0
04	04-24-69		FLARE OCCURS,	DATA DISCONTINUITY		
04	04-26-69	1504.38	1517.90	1536.20	2.173	2.4
04	05-02-69		FLARE OCCURS,	DATA DISCONTINUITY		
04	05-04-69	2049.39	2052.15	2100.26	0.639	1.6
04	05-18-69	1715.31	1723.27	1737.49	46.885	55.4
04	05-18-69	2102.11	2108.25	2121.49	7.095	10.4
04	05-20-69		NO	FLARE		
04	05-28-69		DATA	GAP		
04	05-29-69	1718.14	1728.35	1739.10	3.062	3.8
04	06-05-69	2132.40	2138.41	2201.54	3.847	5.1
04	06-06-69		DATA	GAP		
04	06-06-69	1605.30	1610.28	1713.57	13.702	39.1
04	06-06-69	1953.57	1956.60	2019.54	4.920	5.4

Table 3 (continued)

D. (continued)

	Date	Start	Peak	End	SUMF	Δs
04	06-09-69		NO	FLARE		
04	06-09-69	1206.40	1224.25	1309.20	13.303	6.5
04	06-09-69		NO	FLARE		
04	06-09-69		NO	FLARE		
04	06-09-69		NO	FLARE		
04	06-09-69		NO	FLARE		
04	06-10-69		DATA	GAP		
04	06-10-69	1658.53	1714.32	1724.25	1.217	2.0
04	06-11-69		DATA	GAP		
04	06-12-69		DATA	GAP		
04	06-14-69		DATA	GAP		
04	06-16-69	2021.26	2023.56	2030.45	3.280	6.6
04	06-18-69		1527.46	1553.22	6.858	2.1
04	06-18-69		NO	FLARE		
04	07-05-69	1847.11	1849.31	1852.20	0.191	1.0
04	07-05-69		NO	FLARE		
04	07-14-69		DATA	GAP		
04	07-31-69		DATA	GAP		
04	08-01-69		NO	FLARE		
04	08-10-69		NO	FLARE		
04	08-11-69	1218.21	1221.55	1228.31	9.198	28.1
04	08-11-69		NO	FLARE		
04	08-12-69		DATA	GAP		

Table 4
 Statistical analysis of flux-flux and
 energy-energy relationships.

Correlation Parameters	Correlation Coefficient	Number Data Pairs	Random Data Correlation Coefficient	Confidence
Flux-Flux	0.43	107	0.00 - 0.05	> 99.9%
Flux-Flux (Teske and Thomas, 1969)	0.63	41	0.00 - 0.16	> 99.9%
Energy-Energy	0.14	89	—	< 90.0%

LIST OF REFERENCES

- Acton, L. W.: 1968, "X-Ray and Microwave Emission of the Sun with Special Reference to the Events of July, 1961", Astrophys. J. 152, 305.
- Alfven, H. and Carlqvist, P.: 1967, "Currents in the Solar Atmosphere and a Theory of Solar Flares", Solar Phys. 1, 220.
- Arnoldy, R. L., Kane, S. R., and Winckler, J. R.: 1967, "A Study of Energetic Solar Flare X-Rays", Solar Phys. 2, 171.
- Arnoldy, R. L., Kane, S. R., and Winckler, J. R.: 1968, "The Observations of 10—50 keV Solar Flare X-Rays and Their Correlations with Solar Radio and Energetic Particle Emission", in K. O. Kiepenheuer (ed.), "Structure and Development of Solar Active Regions", IAU Symp. 35, Springer-Verlag, New York.
- Athay, R. D.: 1969, "The Solar Chromosphere", in Frontiers in Astronomy, Readings from Scientific American, W. H. Freeman and Company, San Francisco.
- Carlqvist, P.: 1969, "Current Limitation and Solar Flares", Solar Phys. 7, 377.
- Castelli, J. P. and Aarons, J.: 1968, "The Spectra of Selected Radio Events of March and July, 1966", Annls Geophys. 24, 813.

- Castelli, J. P. and Aarons, J.: 1969, "Spectral Considerations of Microwave Bursts", in C. de Jager (ed.), Solar Flares and Space Research, North Holland, Amsterdam.
- Castelli, J. P. and Guidice, D. A.: 1972, "On the Classification, Distribution, and Interpretation of Solar Microwave Burst Spectra and Related Topics", Air Force Cambridge Research Laboratory Report AFCRL-72-0049.
- Castelli, J. P. and Michel, G.: 1967, "The Sagamore Hill Solar Radio Observatory and the Event of August 28, 1966", Solar Phys. 1, 125.
- Catalano, C.: 1971, "Height Distributions of Soft X-Ray Flares", Ph.D. Thesis, University of Iowa, Iowa City, Iowa.
- Chubb, T. A., Kreplin, R. W., and Friedman, H.: 1966, "Observations of Hard X-Ray Emission from Solar Flares", J. Geophys. Res. 15, 3611.
- Croom, D. L.: 1971, "Solar Microwave Bursts as Indicators of the Occurrence of Solar Proton Emission", Solar Phys. 19, 152.
- Croom, D. L. and Powell, R. J.: 1971, "19 GHz (1.58 cm) Solar Radio Bursts in the Period July 1967 to December 1969", Solar Phys. 20, 136.
- Culhane, J. L. and Phillips, K.: 1970, "Solar X-Ray Burst at Energies of Less than 10 keV Observed with OSO-4", Solar Phys. 11, 117.

- Culhane, J. L., Sanford, P. W., Shaw, M. L., Pounds, K. A., and Smith, D. G.: 1969, "Observations of Solar X-Ray Activity with a Proportional Counter Spectrometer on OSO-IV", in C. De Jager (ed.), Solar Flares and Space Research, North Holland, Amsterdam.
- Culhane, J. L., Vesecky, J. R., and Phillips, K.: 1970, "The Cooling of Flare Produced Plasmas in the Solar Corona", Solar Phys. 15, 394.
- De Jager, C.: 1965, "Solar X-Radiation", Ann. Astrophys. Supp. 28, 263.
- De Jager, C.: 1967a, "The Hard Solar X-Ray Burst of 18 September 1963", Solar Phys. 2, 327.
- De Jager, C.: 1967b, "Note on Solar Hard X-Ray Bursts", Solar Phys. 2, 347.
- De Jager, C.: 1969, "Solar Flares—Properties and Problems", in C. De Jager (ed.), Solar Flares and Space Research, North Holland, Amsterdam.
- Deshpande, S. D. and Tandon, J. N.: 1970, "Soft X-Ray Enhancement During Flares", Solar Phys. 13, 462.
- Drake, J. F.: 1970, "Soft Solar X-Ray Burst Characteristics", Ph.D. Thesis, University of Iowa, Iowa City, Iowa.
- Drake, J. F., Van Allen, J. A., and Gibson, J.: 1969, "Iowa Catalog of Solar Soft X-Ray Flux (2—12 Å)", Solar Phys. 10, 433.
- Elwert, G.: 1961, "Theory of X-Ray Emission of the Sun", J. Geophys. Res. 66, 391.

- Feix, G.: 1969, "Pencilbeam Observations of Solar Bursts at 36 GHz", Solar Phys. 9, 265.
- Friedman, H.: 1969, "X-Ray Observations of Solar Flares", in C. De Jager (ed.), Solar Flares and Space Research, North Holland, Amsterdam.
- Gibson, S. J. and Van Allen, J. A.: 1970, "Correlation of X-Ray Radiation (2-12 Å) with Microwave Radiation from the Non-Flaring Sun", Astrophys. J. 161, 1135.
- Holt, S. S. and Ramaty, R.: 1969, "Microwave and Hard X-Ray Bursts from Solar Flares", Solar Phys. 8, 119.
- Hudson, H. S., Peterson, L. E., and Schwartz, D. A.: 1969a, "The Hard Solar X-Ray Spectrum Observed from the Third Orbiting Solar Observatory", Astrophys. J. 157, 389.
- Hudson, H. S., Peterson, L. E., and Schwartz, D. A.: 1969b, "Solar and Cosmic X-Rays above 7.7 keV", Solar Phys. 6, 205.
- Hudson, H. S., Peterson, L. E., and Schwartz, D. A.: 1969c, "The Time of Solar X-Ray Bursts above 7.7 keV", in C. De Jager (ed.), Solar Flares and Space Research, North Holland, Amsterdam.
- Jackson, J. D.: 1962, Classical Electrodynamics, John Wiley and Sons, New York.
- Kane, S. R.: 1969, "Observations of Two Components in Energetic Solar X-Ray Bursts", Astrophys. J. 157, 139.

- Kane, S. R. and Lin, R. P.: 1972, "Location of the Electron Acceleration Region in Solar Flares", submitted to Solar Phys., University of California, Berkeley, California.
- Kane, S. R. and Winckler, J. R.: 1969, "Observation of Energetic X-Rays and Solar Cosmic Rays Associated with the May 23, 1967 Solar Flare Event", Solar Phys. 6, 304.
- Korchak, A. A.: 1965, "Origin of Hard X-Radiation and of Radio Noise during the Solar Flare of September 28, 1961", Geomagnetism and Aeronomy 5, 21.
- Kraus, J.D.: 1966, Radio Astronomy, McGraw Hill, New York.
- Kreplin, R. W., Moser, P. J. and Castelli, J. P.: 1969, "Flare X-Ray and Radio Wave Emission", in C. De Jager (ed.), Solar Flares and Space Research, North Holland, Amsterdam.
- Kundu, M. R.: 1965, Solar Radio Astronomy, John Wiley and Sons, New York.
- McKenzie, D. L.: 1972, "Correlation Studies of Solar X-Ray and Radio Bursts", Astrophys. J. 175, 481.
- Meekins, J. F., Doskek, G. A., Friedman, H., Chubb, T. A., and Kreplin, R. W.: 1970, "Solar Soft X-Ray Spectra from OSO-4", Solar Phys. 13, 198.
- Milkey, R. W.: 1971, "Comments on the Decay Phase of Impulsive Solar X-Ray Bursts", presented at the 136th AAS Meeting, San Juan, Puerto Rico.
- Neupert, W. M.: 1968, "X-Rays from the Sun", in Leo Goldberg (ed.), Annals and Reviews of Astronomy and Astrophysics, Ann. Reviews, Inc., Palo Alto.

- Ohki, K. I.: 1969, "Directivity of Solar Hard X-Ray Bursts", Solar Phys. 7, 261.
- Parks, G. K. and Winckler, J. R.: 1971, "The Relation of Energetic Solar X-Rays ($h\nu > 60$ keV) and High-Frequency Microwaves Deduced from the Periodic Burst of August 8, 1968 Flare", Solar Phys. 16, 186.
- Sarris, E. T.: 1971, "Study of Solar Flares by the Satellites Explorer 33 and 35", M.S. Thesis, University of Iowa, Iowa City, Iowa.
- Schatzman, E.: 1965, "Particle and Radio Emission from the Sun" in C. De Jager (ed.), The Solar Spectrum, D. Reidel Pub. Corp., Dordrecht, Holland.
- Schwinger, J.: 1949, "On the Classical Radiation of Accelerated Electrons", Phys. Rev. 75,
- Severny, A. B.: 1969, "Solar Flares and B Fields" in C. De Jager (ed.), Solar Flares and Space Research, North Holland, Amsterdam.
- Shimabukuro, F. I.: 1970, "The Observation of 3.3 mm Bursts and Their Correlation with Soft X-Ray Bursts", Solar Phys. 15, 424.
- Smith, D. F. and Priest, E. R.: 1972, "Current Limitation in Solar Flares", Astrophys. J. 176, 487.
- Snidjers, R.: 1968, "Theory of Deka-keV Solar X-Ray Bursts", Solar Phys. 4, 432.

- Snidjers, R.: 1969, "Comments on the X-Ray Event of July 7, 1966",
Solar Phys. 6, 290.
- Spitzer, L.: 1956, Physics of Fully Ionized Gases, Interscience
Publishers Inc., New York.
- Sturrock, P. A. and Coppi, B.: 1966, "A New Model of Solar Flares",
Astrophys. J. 143, 3.
- Svestka, Z.: 1967, "Electron Densities in Flares", Solar Phys. 2, 87.
- Syrovatskii, S. I.: 1969, "On the mechanism of Solar Flares" in
C. De Jager (ed.), Solar Flares and Space Research, North
Holland, Amsterdam.
- Takakura, T.: 1960a, "Synchrotron Radiation from Intermediate
Energy Electrons and Solar Radio Outbursts at Microwave
Frequencies", Pub. Astrophys. Soc. Japan 12, 325.
- Takakura, T.: 1960b, "Synchrotron Radiation for Intermediate Energy
Electrons in Helical Orbits and Solar Radio Bursts at
Microwave Frequencies", Pub. Astrophys. Soc. Japan 12, 352.
- Takakura, T.: 1967, "Theory of Solar Bursts", Solar Phys. 1, 304.
- Takakura, T.: 1969a, "Interpretation of Time Characteristics of
Solar X-Ray Bursts Regering to Associated Microwave Bursts",
Solar Phys. 6, 133.
- Takakura, T.: 1969b, "Flare Associated Radio Bursts" in C. De Jager
(ed.), Solar Flares and Space Research, North Holland,
Amsterdam.

- Takakura, T.: 1969c, "Interpretation of Time Characteristics of Solar X-Ray Bursts", in C. De Jager (ed.), Solar Flares and Space Research, North Holland, Amsterdam.
- Takakura, T. and Kai, K.: 1966, "Energy Distribution of Electrons Producing Microwave Impulsive Bursts and X-Ray Burst from the Sun", Pub. Astrophys. Soc. Japan 18, 57.
- Takakura, T., Uchida, Y., and Kai, K.: 1968, "Time Variation of Spectrum of Gyro-Synchrotron Radiation from the Sun", Solar Phys. 4, 45.
- Tanaka, T. Kakinuma, T., and Enome, S.: 1968, "High Resolution Observations of Solar Radio Bursts with Multi-Element Compound Interferometer at 3.75 and 9.4 GHz", Solar Phys. 6, 428.
- Teske, R. G. and Thomas, R. J.: 1969, "Soft Solar X-Rays and Solar Activity I; Relationships Between Reported Flare and Radio Bursts and X-Ray Bursts", Solar Phys. 8, 348.
- Thomas, R. J. and Teske, R. G.: 1971, "Solar Soft X-Rays and Solar Activity II; Soft X-Ray Emission During Solar Flares", Solar Phys. 16, 431.
- Underwood, J. H.: 1968, "Solar X-Rays", Science 159, 383.
- Van Allen, J. A.: 1967, "The Solar X-Ray Flare of July 7, 1966", J. Geophys. Res. 72, 5903.
- Van Allen, J. A. and Ness, N. F.: 1967, "Observed Particle Events of an Interplanetary Shock Wave of July 8, 1968", J. Geophys. Res. 72, 935.

- Van De Hulst, H. C.: 1950, "The Electron Density of the Solar Corona", B.A.N. 11, 135.
- Vorpahl, J.: 1972, "X-Radiation ($E > 10$ keV) H α and Microwave Emission During the Impulsive Phase of Solar Flares", submitted to Solar Phys., University of California, Berkeley, California.
- Wende, C. D.: 1968, "The Correlation of Solar Microwave and Soft X-Ray Radiation", Ph.D. Thesis, University of Iowa, Iowa City, Iowa.
- Young, H. D.: 1962, Statistical Treatment of Experimental Data, McGraw Hill, New York.
- Zirin, H., Pruss, G., and Vorpahl, J.: 1971, "Magnetic Fields, Bremsstrahlung and Synchrotron Emission in the Flare of 24 October 1969", Solar Phys. 19, 463.

LIST OF FIGURES

- Figure 1 A model of the solar atmosphere.
- Figure 2 The types of centimetric wavelength solar bursts. (After Kundu, 1965)
- Figure 3 A compound model of the solar flare region. The microwave impulsive burst occurs in the regions noted R_1 and R_2 , where the plasma density is low but the magnetic field is high. The source of hard x-ray emission is the region marked X. (After Takakura, 1969b)
- Figure 4 A non-compound model of the solar flare region. In this model the hard x-ray radiation and the microwave radiation would occur at the same location. The model is consistent with observational evidence that impulsive bursts occur at altitudes of approximately 6000 km. (After Vorpahl, 1972)
- Figure 5 The solar soft x-ray flux as observed by Explorer 33 on July 26, 1967.
- Figure 6 The solar soft x-ray flux as observed by Explorer 35 on December 3, 1967.
- Figure 7 The microwave burst types. Classification is made on the basis of duration and flux change. (After Kundu, 1965)

- Figure 8 A solar flare with associated microwave and x-ray emission occurring on November 2, 1968. The trace at the bottom of the page represents a microwave flux as recorded at the NLRO. The points represent 82-sec averages of solar soft x-ray flux. The number in parentheses indicates flux change as measured at Sagamore Hill. The number outside the parentheses is flux change as measured at the NLRO.
- Figure 9 A solar flare with associated microwave and x-ray emission occurring on March 21, 1969. The trace at the bottom of the page represents a microwave flux as recorded at the NLRO. The points represent 82-sec averages of solar soft x-ray flux. The number in parentheses indicates flux change as measured at Sagamore Hill. The number outside the parentheses is flux change as measured at the NLRO. The multiple peaks at the peak of the x-ray event are due to a satellite spin effect.
- Figure 10 A solar flare with associated microwave and x-ray emission occurring on July 3, 1969. The trace at the bottom of the plot represents a microwave flux as recorded at the NLRO. The points represent 82-sec averages of solar soft x-ray flux. The number in parentheses indicates flux change as measured at Sagamore Hill. The number outside the parentheses is flux change as measured at the NLRO.
- Figure 11 A plot of flux change versus duration for all microwave flares for which these data were available.

- Figure 12 A histogram of impulsiveness index for microwave bursts. Index of impulsiveness is defined as flare flux change over flare duration.
- Figure 13 A histogram of microwave flare durations.
- Figure 14 A histogram of values for microwave peak flux time minus x-ray peak flux time. A negative value indicates that the x-ray peak flux time preceded the microwave peak flux time.
- Figure 15 A histogram of values for microwave flare start time minus x-ray flare start time. A negative value indicates that the x-ray emission preceded the microwave emission.
- Figure 16 Microwave flare flux change (intensity) versus x-ray flare flux change. The radio flux change is measured in solar flux units; the x-ray flux change is measured in $\text{erg sec}^{-1} \text{cm}^{-2}$. The line represents a least squares fit to the data.
- Figure 17 A plot of time-integrated flux over duration of flare for the microwave flare versus the same quantity for the x-ray flare. This plot compares the total energy received at earth from the flare in the x-ray and microwave regions.
- Figure 18 The model for the electron acceleration mechanism. (See text.)
- Figure 19 A histogram of values for microwave end time minus x-ray peak time.

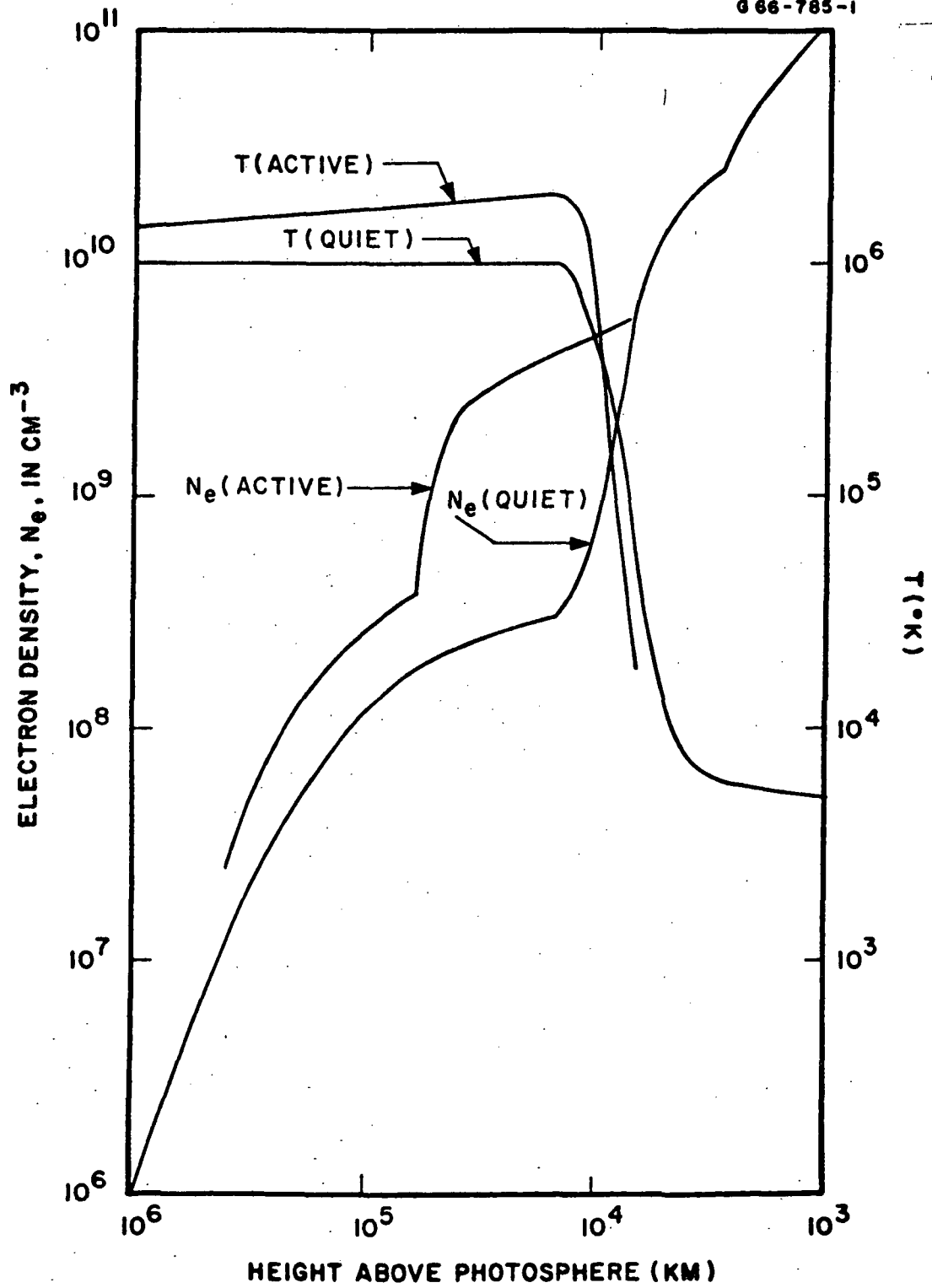


Figure 1






Example	Type	Description (Covington)	Duration (Min.)	Polarization	Source Angular Size (min. arc)	Max. Equiv. Temp.	Radiation Mechanism
	Type A	Simple burst-impulsive	1 to 5	Random or partially circular; sometimes linear	<2.5	$\sim 10^6$ to 10^8 °K	Synchrotron or nonthermal bremsstrahlung
	Type B	Post burst-slow decay	10 to 200	Random or partially circular; sometimes linear	>3'	$\sim 10^6$ to 10^7 °K	Probably thermal
	Type C	Gradual rise and fall	10 to 100	Partially circular	<1'	$\sim 10^6$ °K	Same as slowly varying component.
		Absorption following burst	10 to 100	?	?	?	Thermal
		Fluctuations	30 to 150	?	?	?	Apparently due to absorption of the slowly varying radiation by an overlying dense gas cloud.

Figure 2

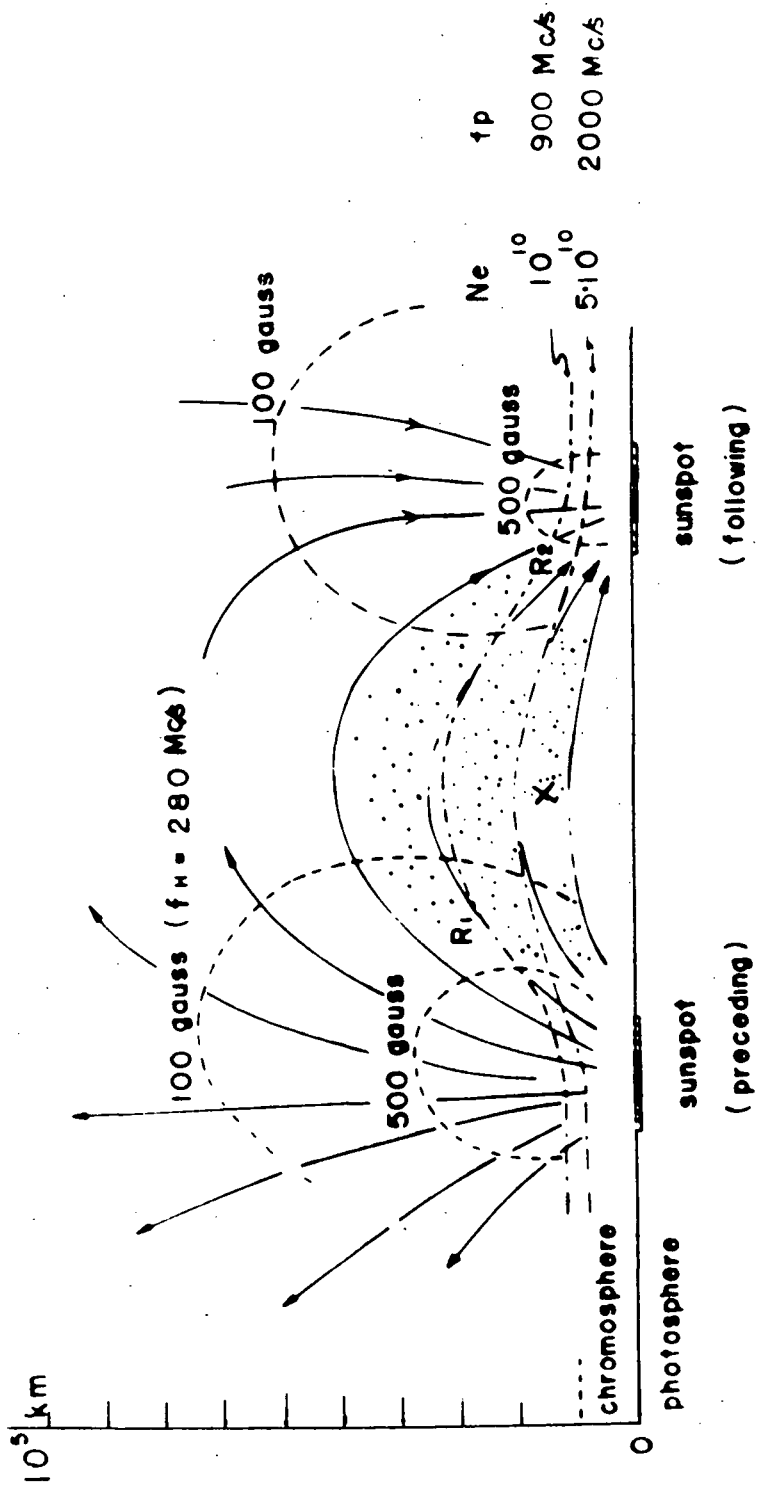


Figure 3

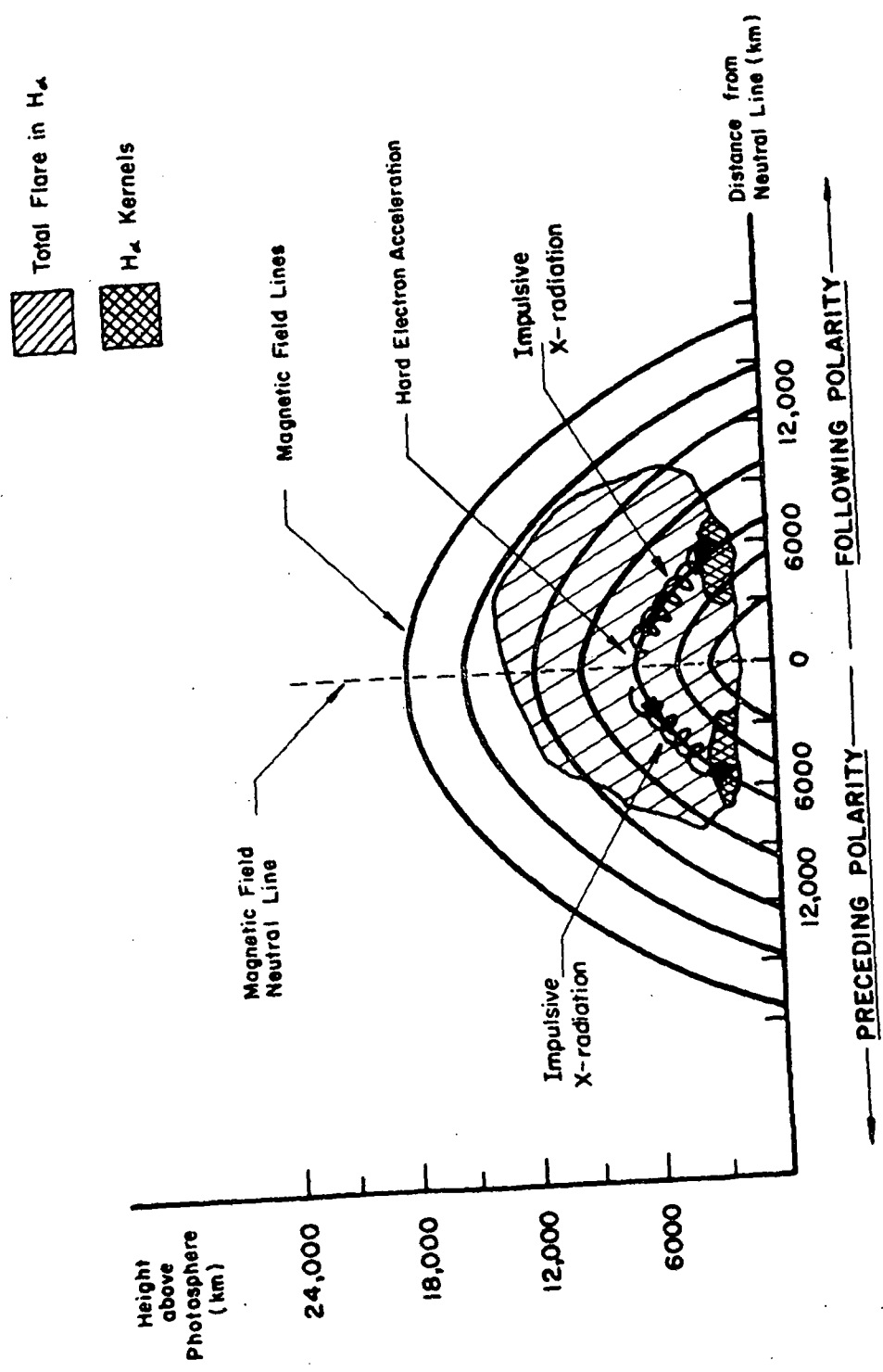


Figure 4

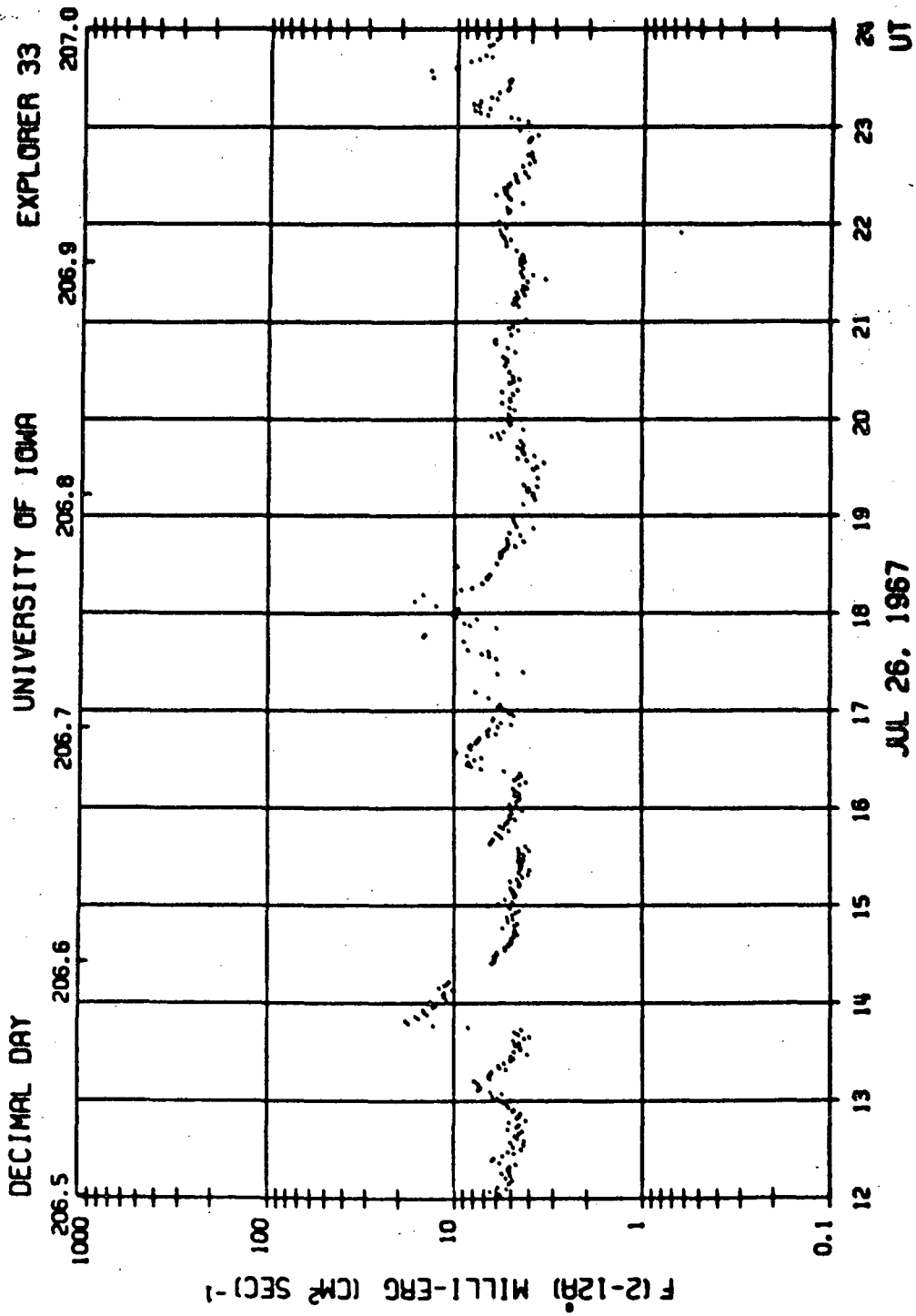


Figure 5

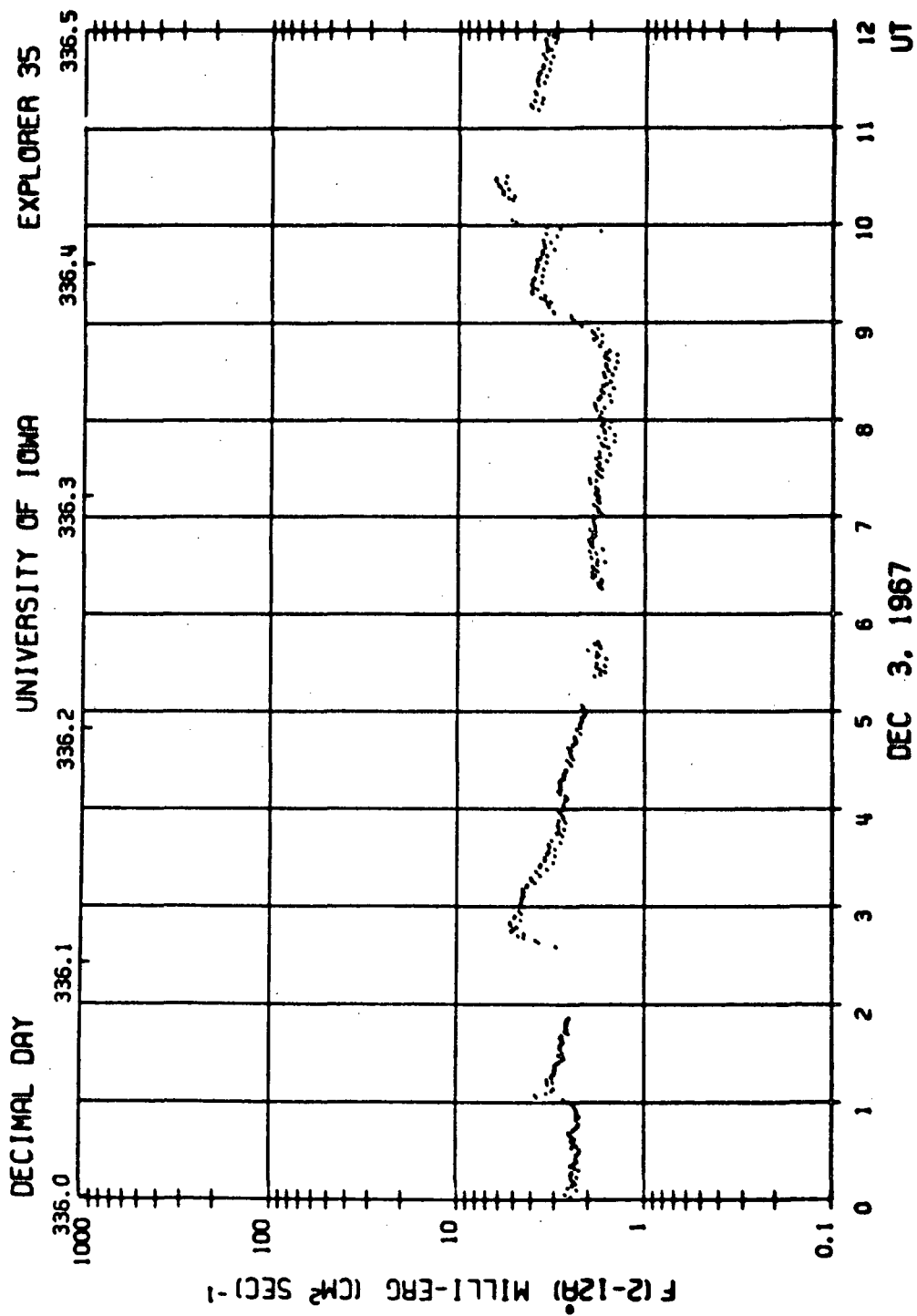
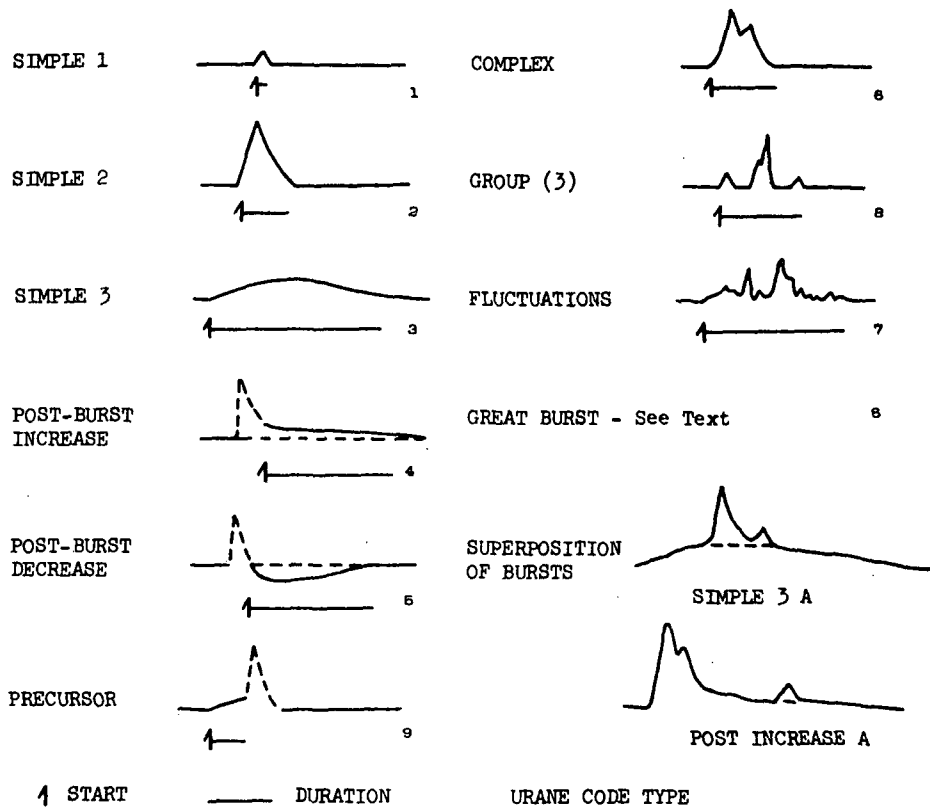
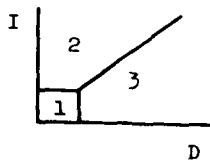


Figure 6



RELATION OF SIMPLE BURSTS TO DIAGRAM OF INTENSITY VERSUS DURATION



Region 1 - SIMPLE 1: Intensity ≤ 7.5 flux units
Duration ≤ 7.5 minutes
May be impulsive

Region 2 - SIMPLE 2: Intensity > 7.5 flux units
Impulsive

Region 3 - SIMPLE 3: Duration > 7.5 minutes
Long Enduring (Gradual Rise and Fall)

FLUX UNIT 10^{-22} watts/m²/c/s

Figure 7

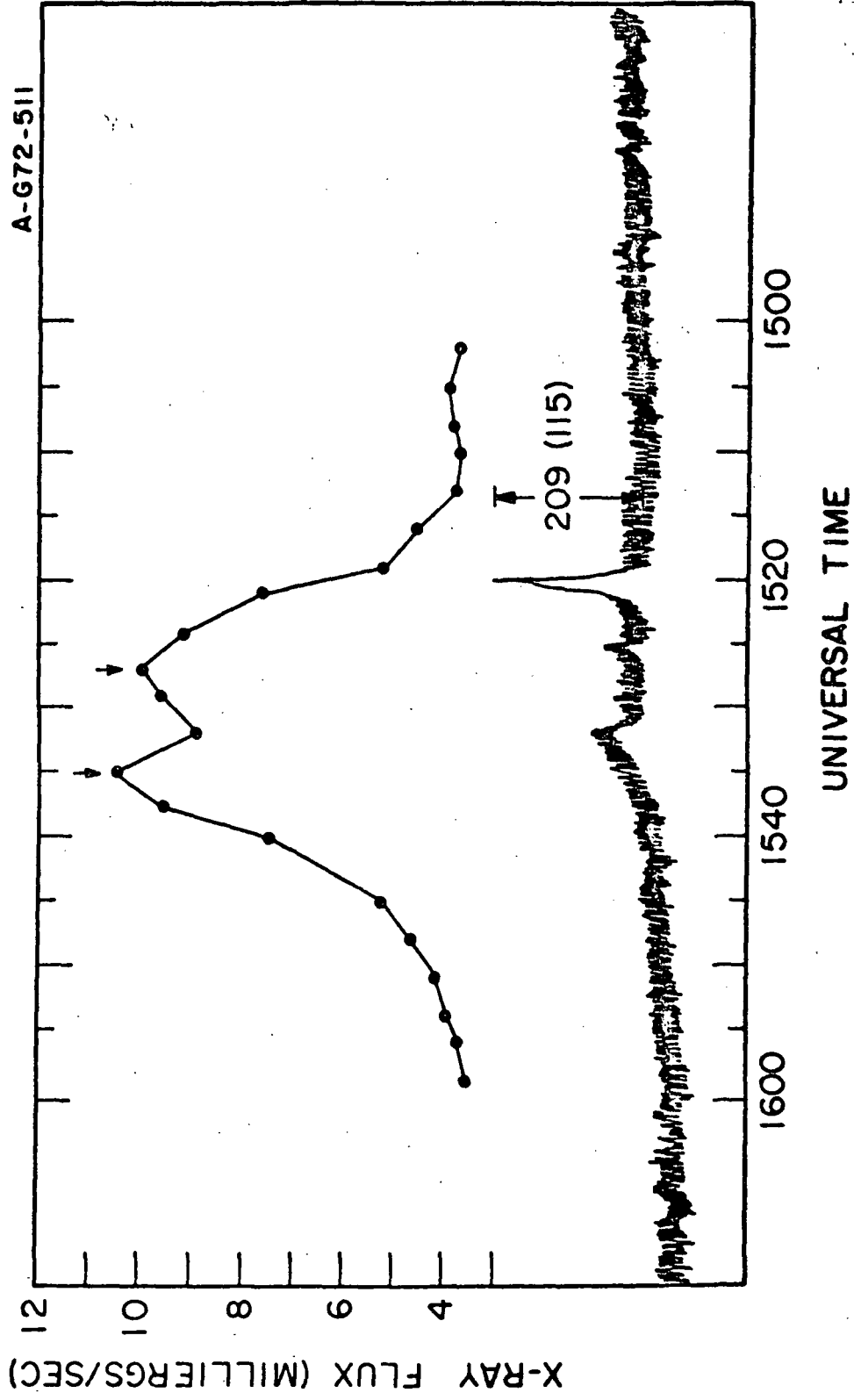


Figure 8

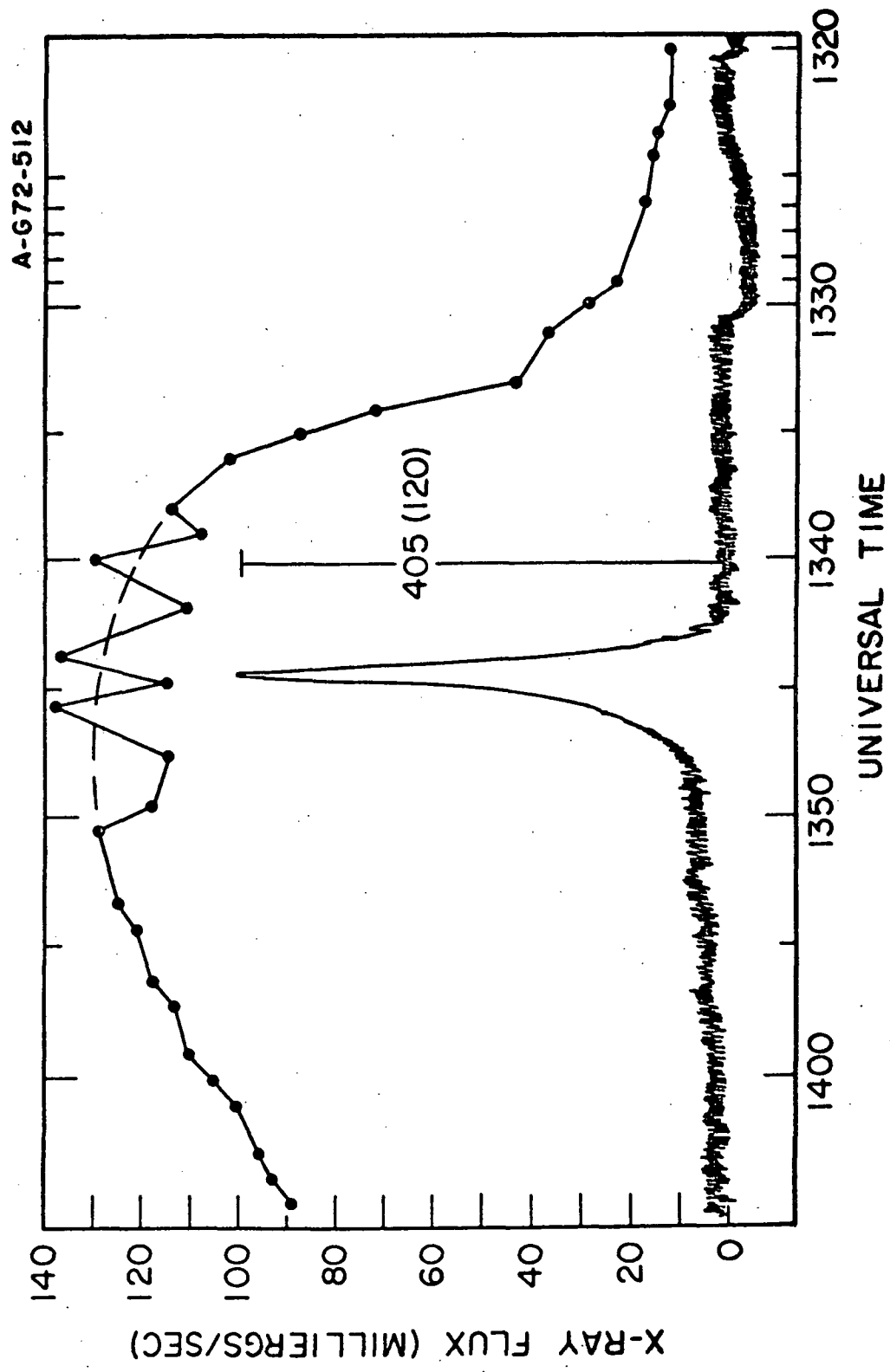
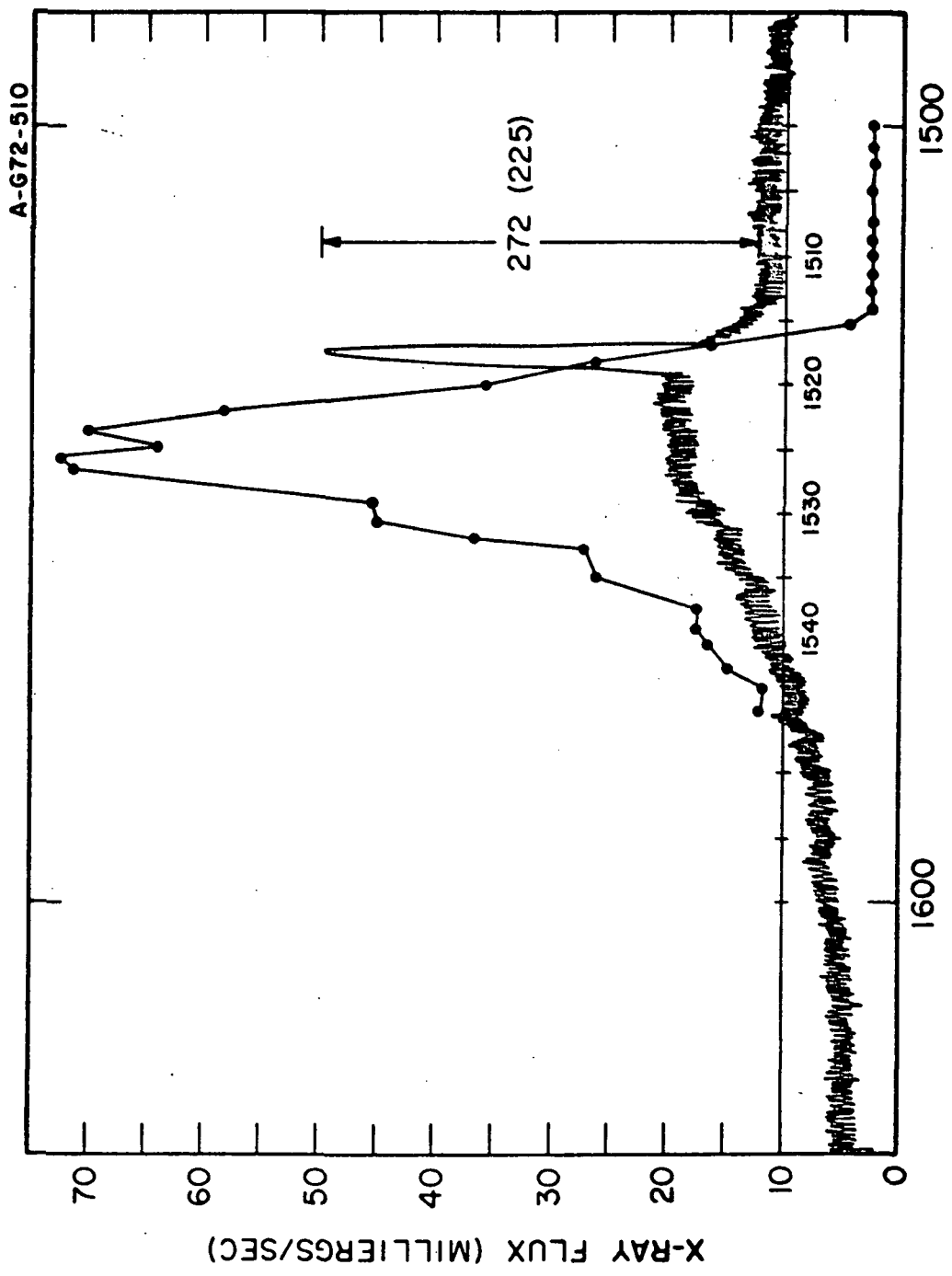


Figure 9



JULY 3, 1969 - 1510
 UNIVERSAL TIME

Figure 10

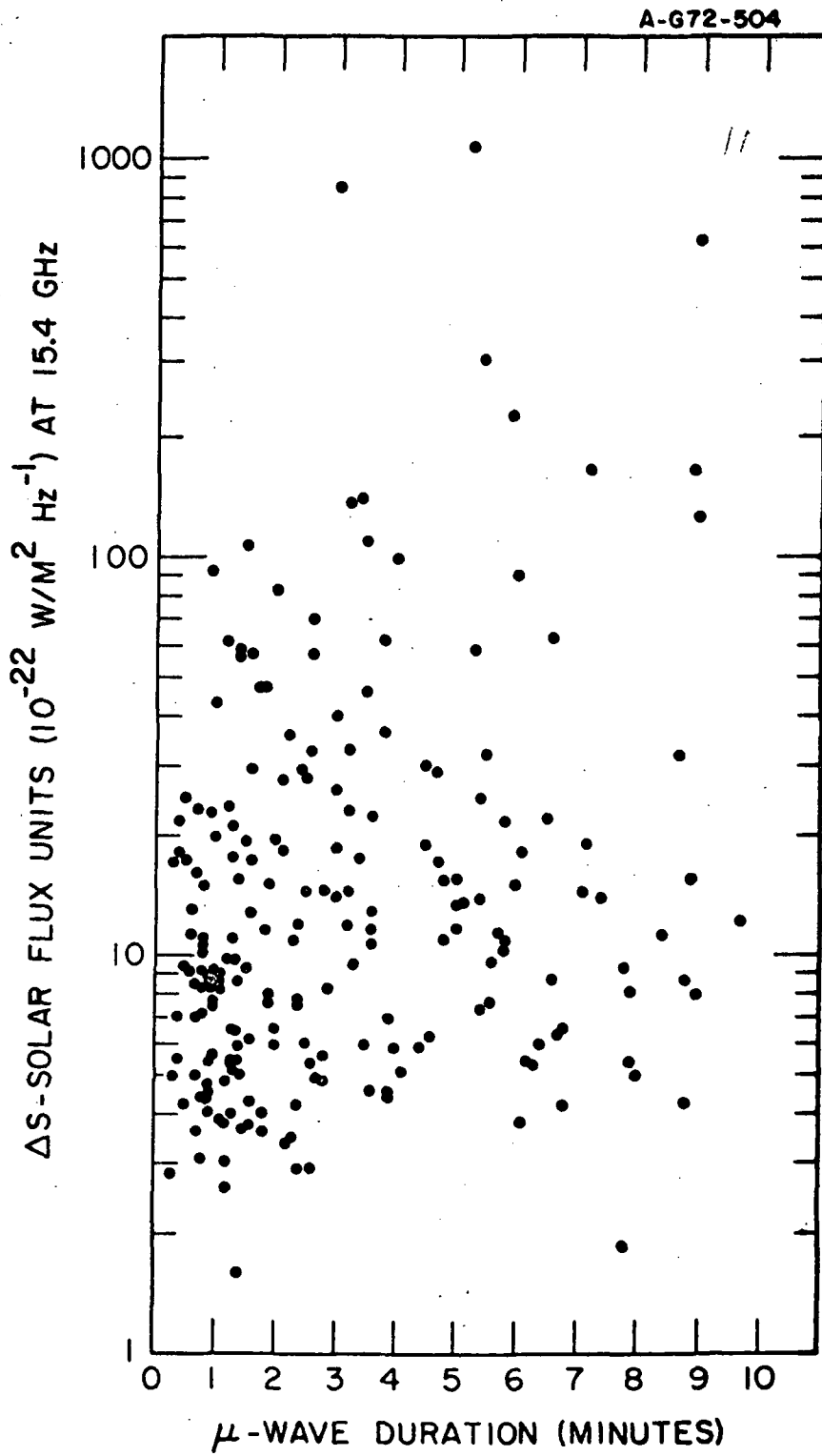


Figure 11

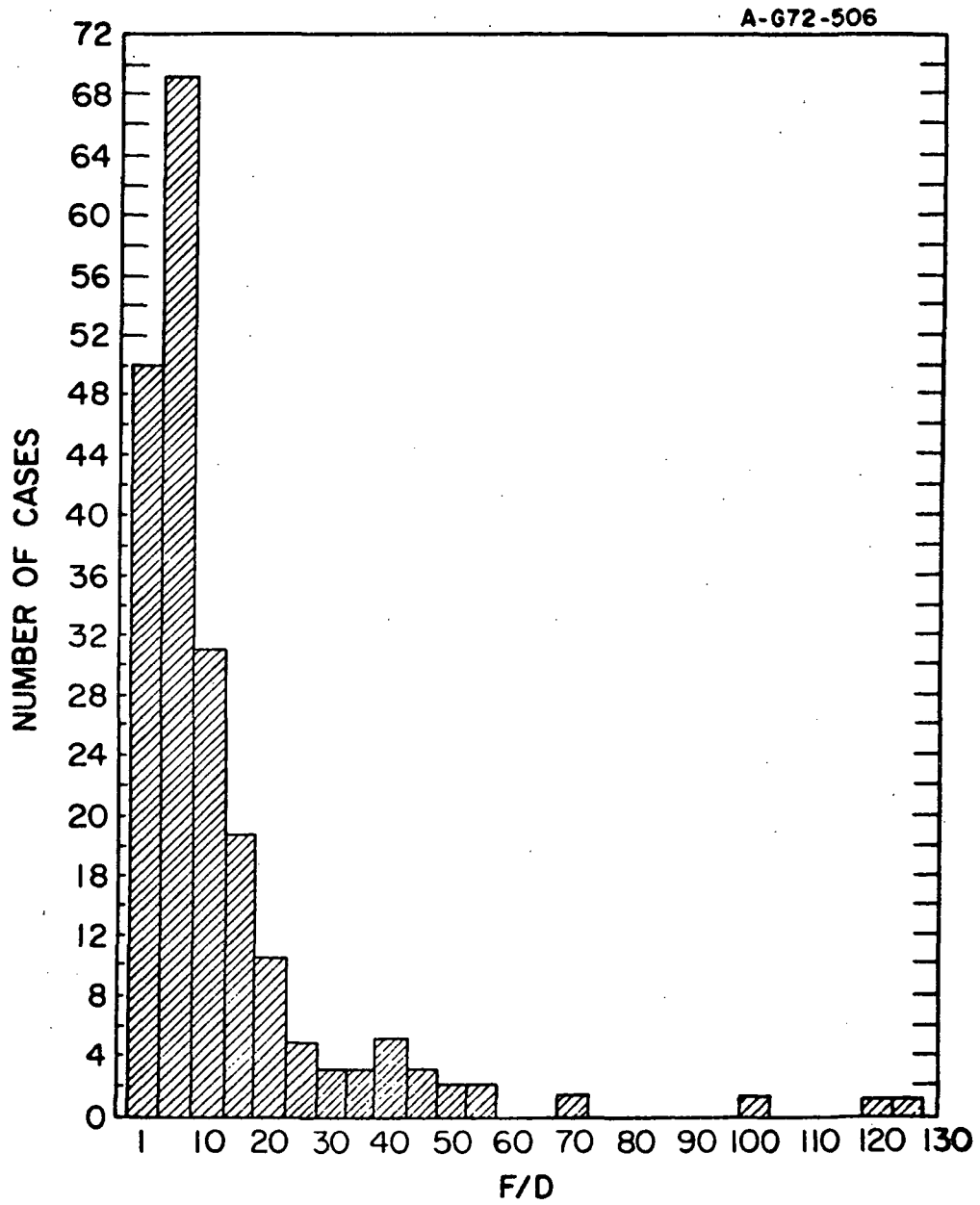


Figure 12

A-G72-697

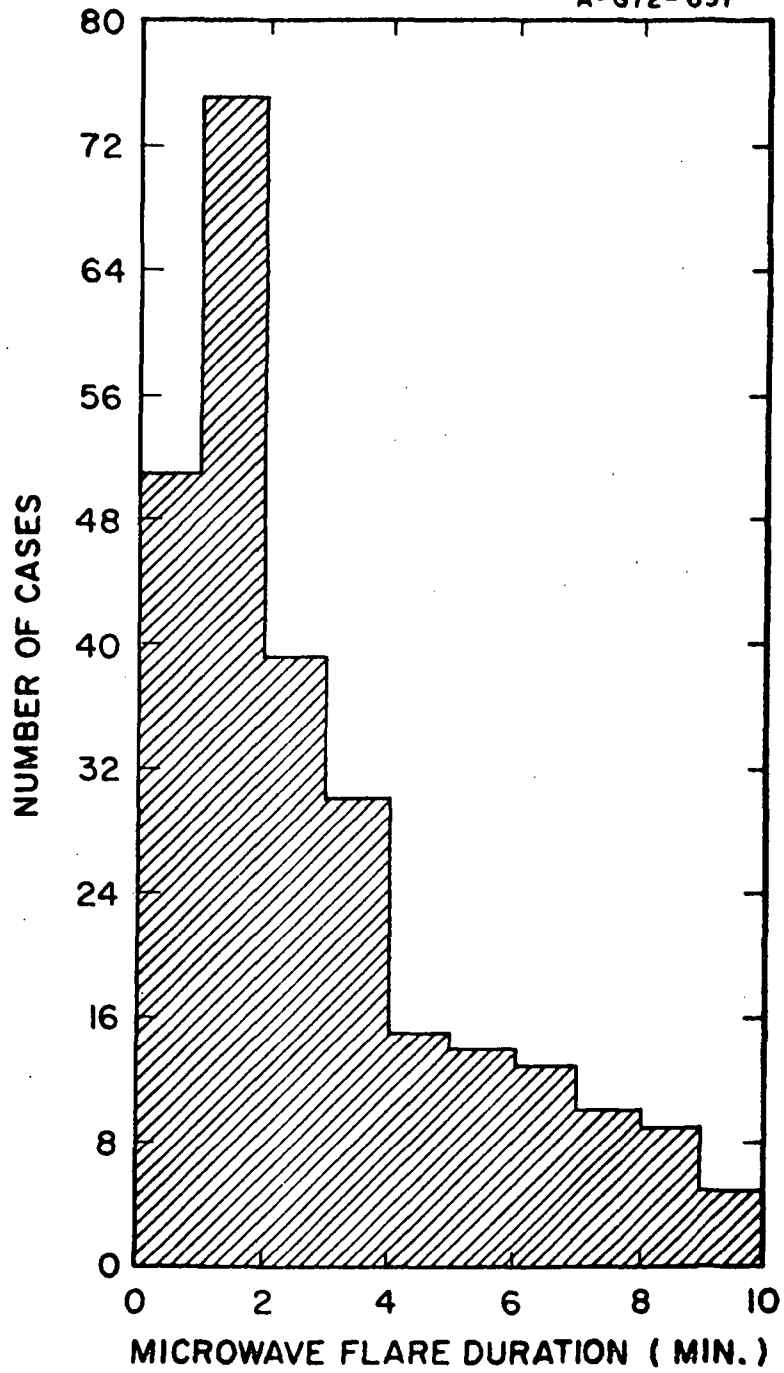


Figure 13

C2

A-672-507

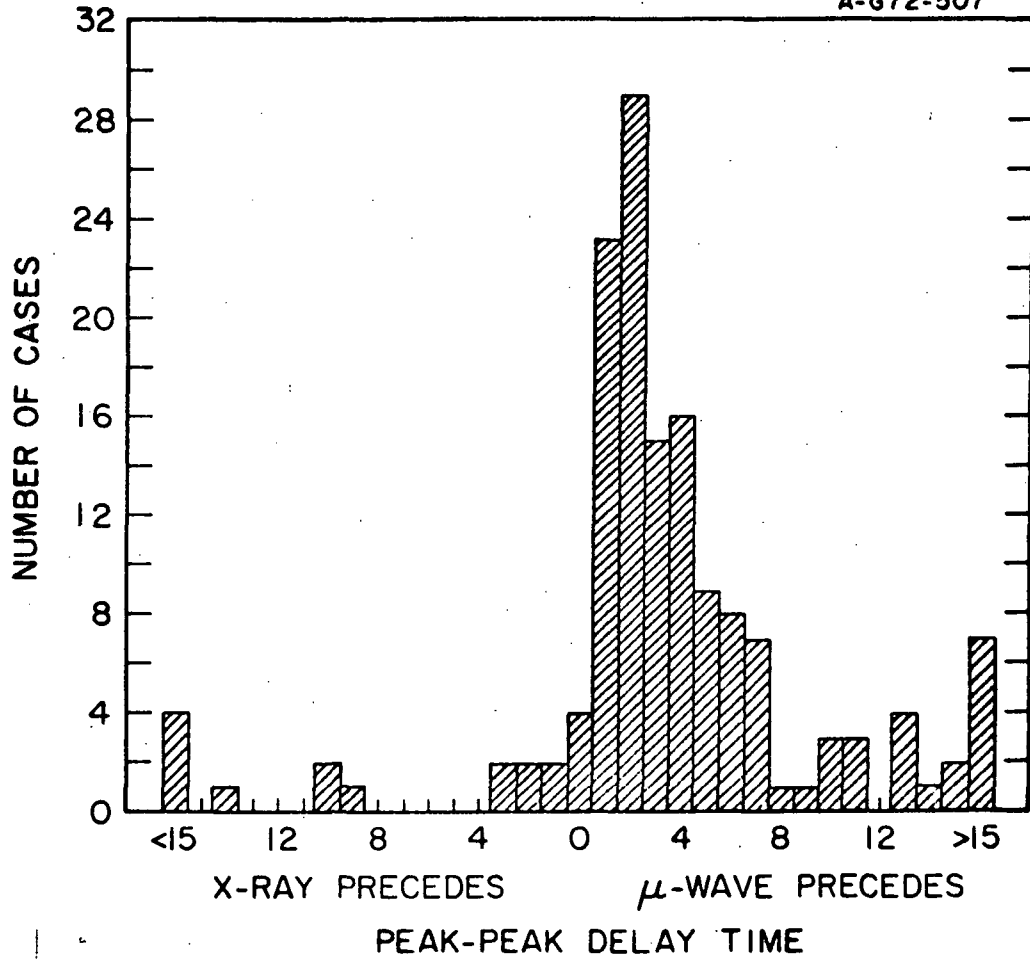


Figure 14

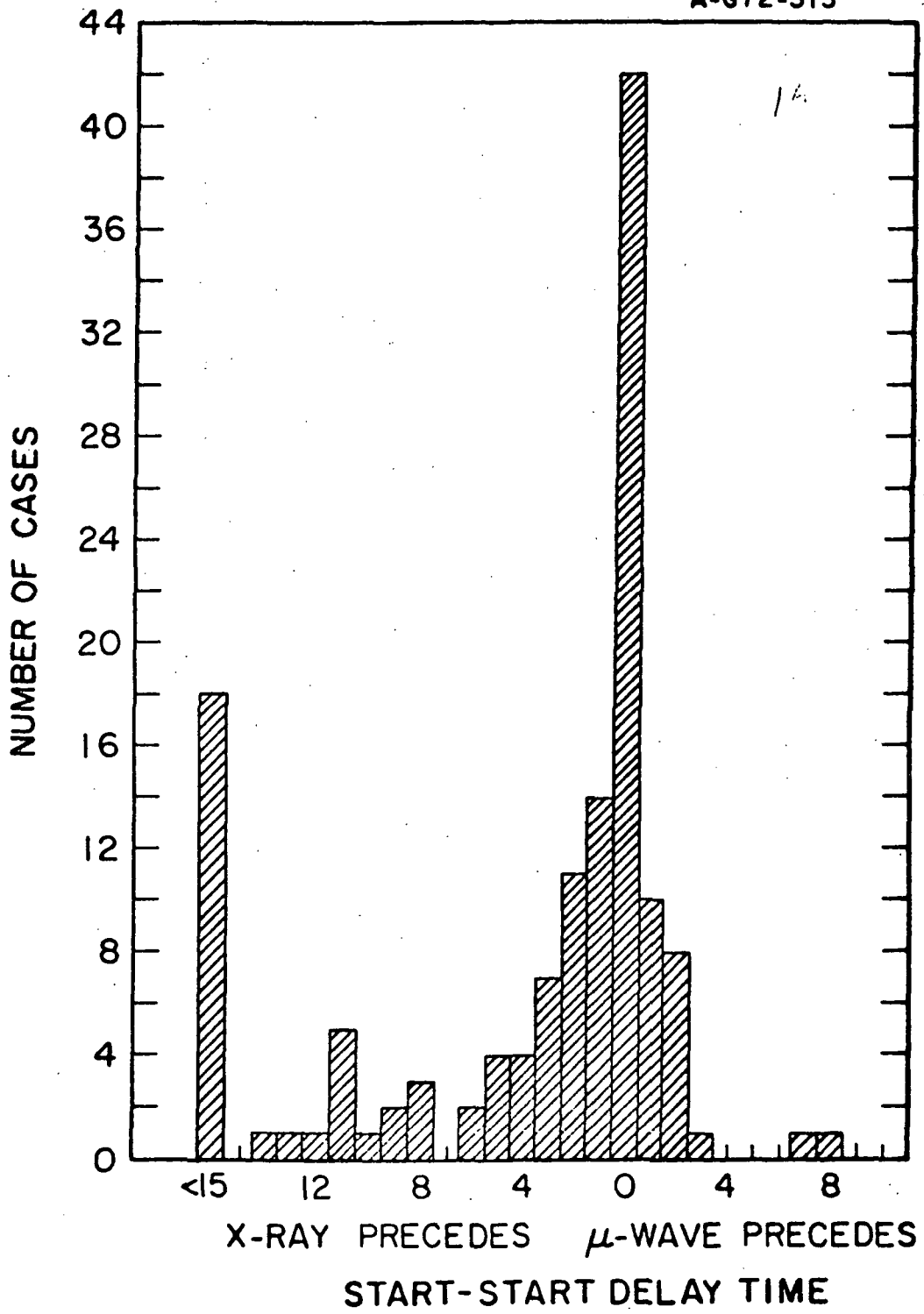


Figure 15

A-672-515

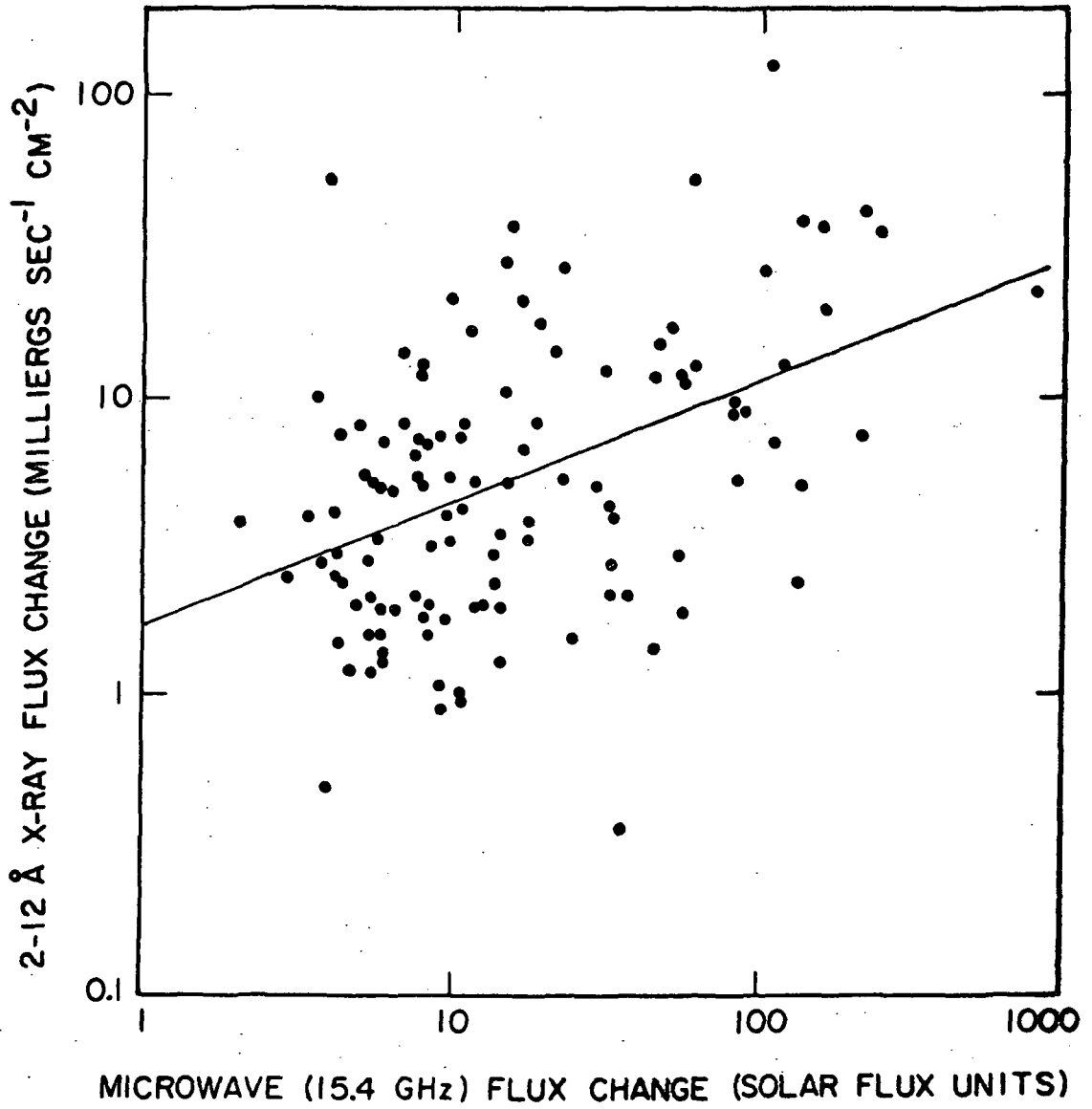


Figure 16

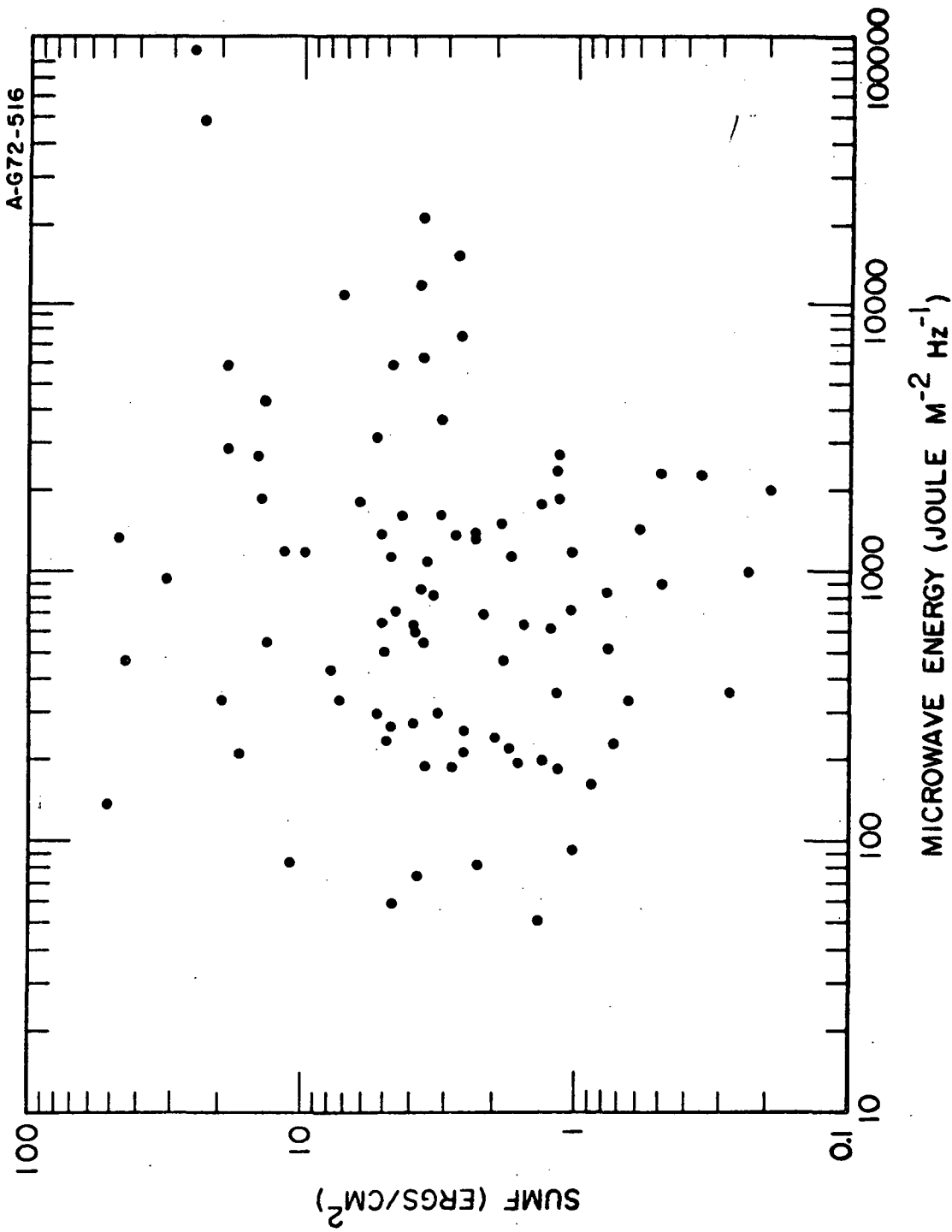


Figure 17

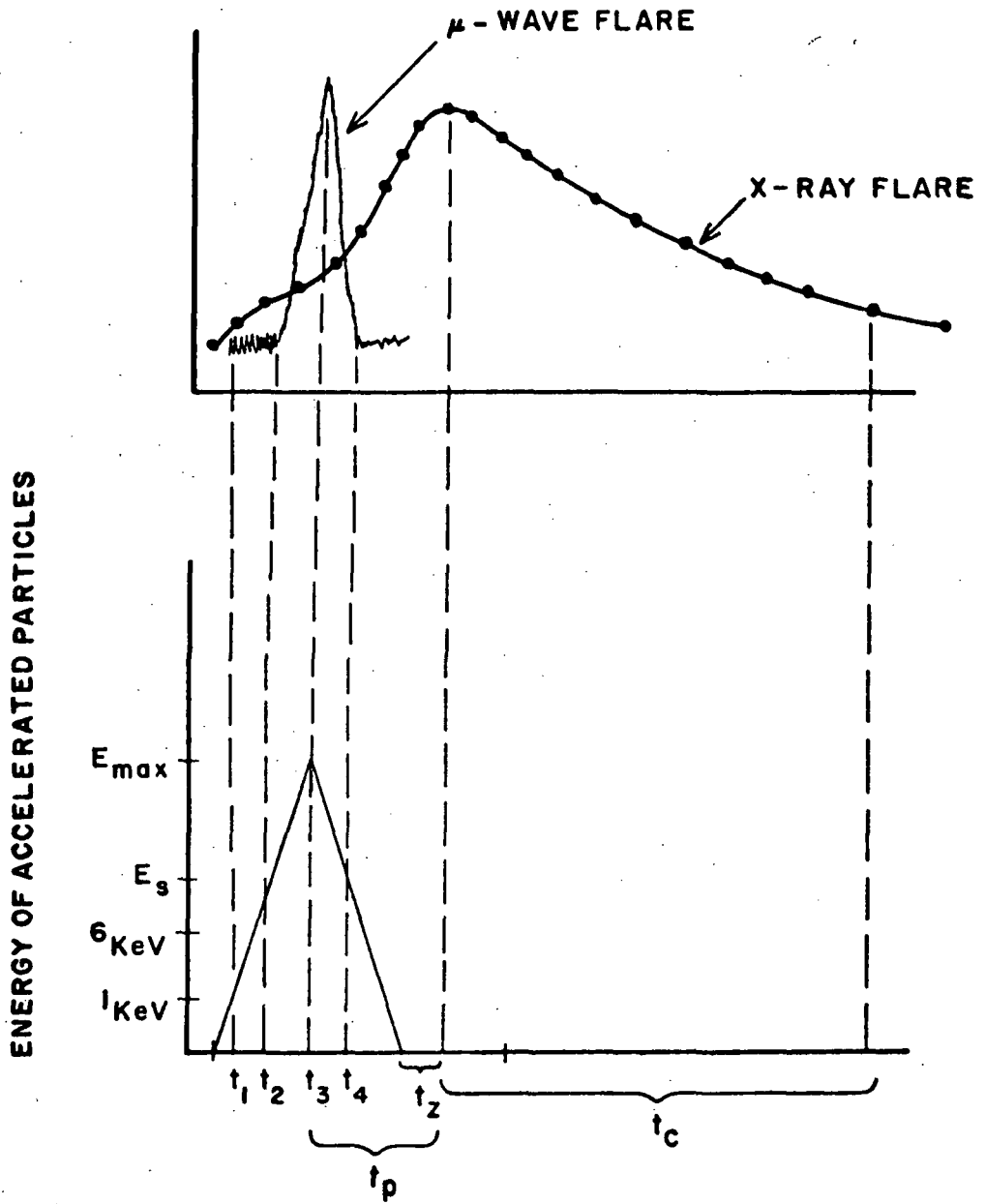


Figure 18

A-672-666

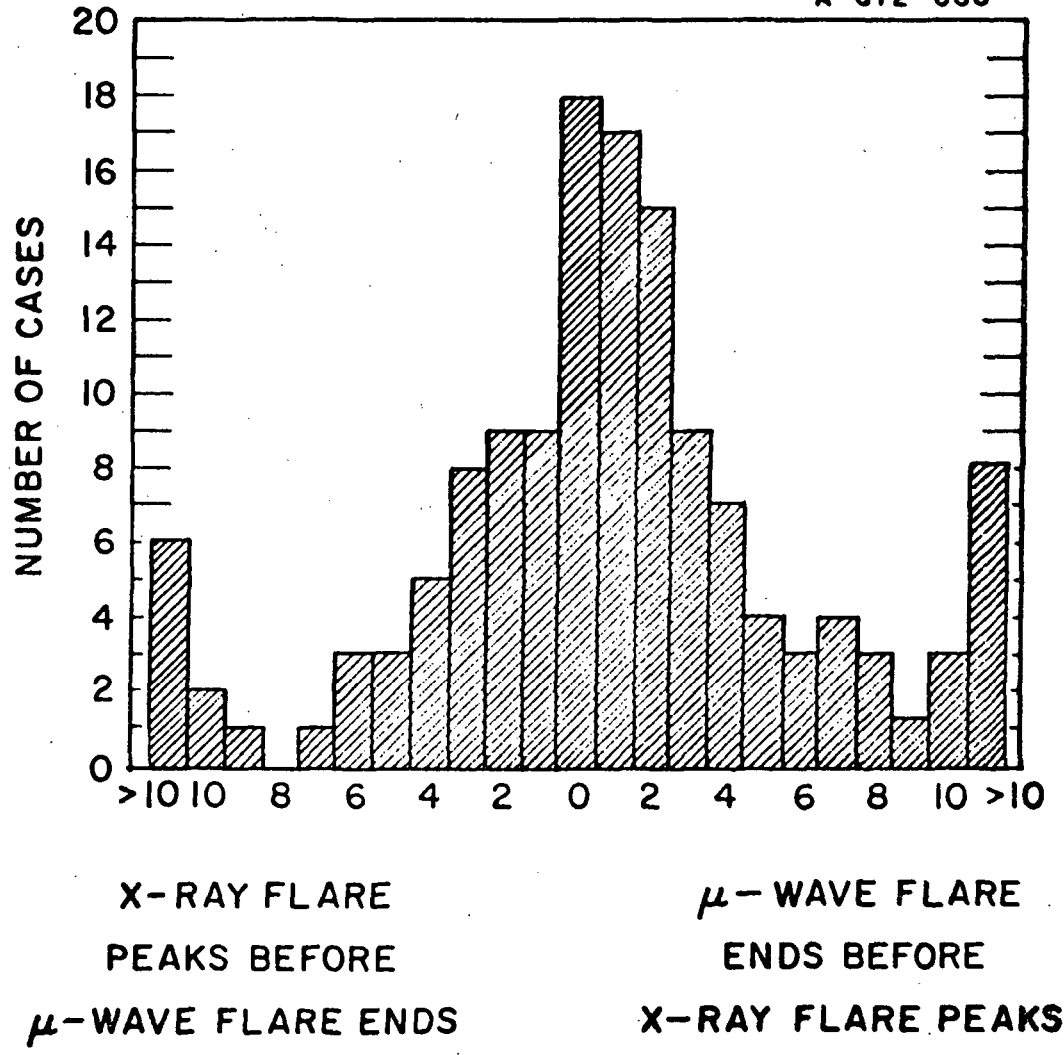


Figure 19

DOCUMENT CONTROL DATA - R&D

(Security classification of title, body of abstract and indexing annotation must be entered when the overall report is classified)

1. ORIGINATING ACTIVITY (Corporate author) Department of Physics and Astronomy University of Iowa Iowa City, Iowa 52242		2a. REPORT SECURITY CLASSIFICATION Unclassified	
		2b. GROUP	
3. REPORT TITLE Short-Duration Solar Microwave Bursts and Associated Soft X-ray Emission			
4. DESCRIPTIVE NOTES (Type of report and inclusive dates) M.S. thesis, December 1972			
5. AUTHOR(S) (Last name, first name, initial) Spangler, Steven R.			
6. REPORT DATE December 1972	7a. TOTAL NO. OF PAGES 127	7b. NO. OF REFS 77	
8a. CONTRACT OR GRANT NO. N00014-68-A-0196-003	9a. ORIGINATOR'S REPORT NUMBER(S) U. of Iowa 73-2		
b. PROJECT NO.	9b. OTHER REPORT NO(S) (Any other numbers that may be assigned this report)		
c.			
d.			
10. AVAILABILITY/LIMITATION NOTICES Distribution is unlimited			
11. SUPPLEMENTARY NOTES		12. SPONSORING MILITARY ACTIVITY	
13. ABSTRACT See following pages.			

14. KEY WORDS	LINK A		LINK B		LINK C	
	ROLE	WT	ROLE	WT	ROLE	WT
Microwave Impulsive Bursts Soft X-rays						

INSTRUCTIONS

1. ORIGINATING ACTIVITY: Enter the name and address of the contractor, subcontractor, grantee, Department of Defense activity or other organization (*corporate author*) issuing the report.

2a. REPORT SECURITY CLASSIFICATION: Enter the overall security classification of the report. Indicate whether "Restricted Data" is included. Marking is to be in accordance with appropriate security regulations.

2b. GROUP: Automatic downgrading is specified in DoD Directive 5200.10 and Armed Forces Industrial Manual. Enter the group number. Also, when applicable, show that optional markings have been used for Group 3 and Group 4 as authorized.

3. REPORT TITLE: Enter the complete report title in all capital letters. Titles in all cases should be unclassified. If a meaningful title cannot be selected without classification, show title classification in all capitals in parenthesis immediately following the title.

4. DESCRIPTIVE NOTES: If appropriate, enter the type of report, e.g., interim, progress, summary, annual, or final. Give the inclusive dates when a specific reporting period is covered.

5. AUTHOR(S): Enter the name(s) of author(s) as shown on or in the report. Enter last name, first name, middle initial. If military, show rank and branch of service. The name of the principal author is an absolute minimum requirement.

6. REPORT DATE: Enter the date of the report as day, month, year; or month, year. If more than one date appears on the report, use date of publication.

7a. TOTAL NUMBER OF PAGES: The total page count should follow normal pagination procedures, i.e., enter the number of pages containing information.

7b. NUMBER OF REFERENCES: Enter the total number of references cited in the report.

8a. CONTRACT OR GRANT NUMBER: If appropriate, enter the applicable number of the contract or grant under which the report was written.

8b, 8c, & 8d. PROJECT NUMBER: Enter the appropriate military department identification, such as project number, subproject number, system numbers, task number, etc.

9a. ORIGINATOR'S REPORT NUMBER(S): Enter the official report number by which the document will be identified and controlled by the originating activity. This number must be unique to this report.

9b. OTHER REPORT NUMBER(S): If the report has been assigned any other report numbers (*either by the originator or by the sponsor*), also enter this number(s).

10. AVAILABILITY/LIMITATION NOTICES: Enter any limitations on further dissemination of the report, other than those

imposed by security classification, using standard statements such as:

- (1) "Qualified requesters may obtain copies of this report from DDC."
- (2) "Foreign announcement and dissemination of this report by DDC is not authorized."
- (3) "U. S. Government agencies may obtain copies of this report directly from DDC. Other qualified DDC users shall request through _____."
- (4) "U. S. military agencies may obtain copies of this report directly from DDC. Other qualified users shall request through _____."
- (5) "All distribution of this report is controlled. Qualified DDC users shall request through _____."

If the report has been furnished to the Office of Technical Services, Department of Commerce, for sale to the public, indicate this fact and enter the price, if known.

11. SUPPLEMENTARY NOTES: Use for additional explanatory notes.

12. SPONSORING MILITARY ACTIVITY: Enter the name of the departmental project office or laboratory sponsoring (*paying for*) the research and development. Include address.

13. ABSTRACT: Enter an abstract giving a brief and factual summary of the document indicative of the report, even though it may also appear elsewhere in the body of the technical report. If additional space is required, a continuation sheet shall be attached.

It is highly desirable that the abstract of classified reports be unclassified. Each paragraph of the abstract shall end with an indication of the military security classification of the information in the paragraph, represented as (TS), (S), (C), or (U).

There is no limitation on the length of the abstract. However, the suggested length is from 150 to 225 words.

14. KEY WORDS: Key words are technically meaningful terms or short phrases that characterize a report and may be used as index entries for cataloging the report. Key words must be selected so that no security classification is required. Identifiers, such as equipment model designation, trade name, military project code name, geographic location, may be used as key words but will be followed by an indication of technical content. The assignment of links, roles, and weights is optional.